R83-2

SOLAR POND FEASIBILITY STUDY FOR EGYPT
– PRELIMINARY REPORT –

by

Atul Salhotra
E. Eric Adams
Donald R.F. Harleman

RALPH M. PARSONS LABORATORY
AQUATIC SCIENCE AND ENVIRONMENTAL ENGINEERING

Report No. 288

Prepared under the support of the
Technology Adaptation Program
Agency for International Development

JANUARY 1983

DEPARTMENT
OF
CIVIL
ENGINEERING

SCHOOL OF ENGINEERING
MASSACHUSETTS INSTITUTE OF TECHNOLOGY
Cambridge, Massachusetts 02139

ACKNOWLEDGEMENTS

This work was sponsored by the M.I.T. Technology Adaptation Program which is funded through a grant from the Agency for International Development, United States Department of State.

Acknowledgements are due to the Technology Planning Program which includes personnel at M.I.T. and Cairo University. Their administrative support and cooperation has been very helpful.

Thanks are due to Mrs. Carole Solomon who typed this report.

ABSTRACT

The report presents a preliminary feasibility study for salt gradient solar ponds in Egypt. Chapter 1 gives a brief review of the technical and economic aspects of solar ponds. Chapter 2 includes a discussion of the ongoing analytical and experimental research at the Ralph M. Parsons Laboratory. Chapter 3 investigates the potential and technical feasibility of construction and operation of large scale solar ponds in the Qattara Depression. Performance of the proposed solar ponds has been simulated using the Solar Pond Model developed at M.I.T. Chapter 4 gives details of the construction, operation and performance of small demonstration solar ponds at Lake Qarun or Lake Maruit.

TABLE OF CONTENTS

1. A Brief Review of Salt Gradient Solar Ponds

Introduction

The solar pond is a natural method for the large scale utilization of solar energy. In recent years a number of these ponds have been constructed in different parts of the world. Ponds ranging from a few m^2 to a few thousand m^2 in area are successfully in operation in the USA, Israel and Australia. Table 1.1 lists characteristics of a few ponds in operation and those proposed to be constructed in the next few years. Experience gained from the operating ponds has proven the technical feasibility of solar ponds as large-scale energy collectors and storage units. The generation of electricity from Yavne and Ein Bokek ponds in Israel (1) has advanced the technology to a point where it can be referred to as proven technology.

There now exists an extensive literature on solar ponds. In November 1981, the Solar Energy Information Data Bank operated by the U.S. Department of Energy published a selected bibliography containing over 250 references on the subject (25). The purpose of this chapter is to review the subject of solar ponds in the light of experience gained from ponds actually built or conceived (Table 1.1). A more comprehensive treatment may be obtained from the extensive list of references.

Structure of a Solar Pond

A solar pond is a shallow body of water with three fairly distinct zones (Figure 1.1). The topmost layer or the upper convecting zone (UCZ)

Table 1.1 Solar Ponds in Operation and Proposed

LOCATION	DATE COMPLETED	DIMENSION	PURPOSE	COST (installation)
Yavne, Israel	1977	1500 m^2	Research. 6KWe power generated	
Ein Bokek, Israel	Dec. 1979	7000 m^2 3 m deep	Research 150 KWe peak power operation	
Miamisburg, Ohio, USA	1978	2000 m^2 3 m deep	Heating an indoor swimming pool	$70,000
Ohio State Univ., Ohio	Aug. 1975	200 m^2 2.5 m deep	Study and possible commercialization	$7,500 Exclusive of research equipment. Salt - $2,400 Liner - $2,500
Argonne National Laboratory, Illinois, USA	Nov. 1980	1080m^2 43 m x 25 m x 4.3 m	Research	
University of New Mexico, USA	Fall 1975	15 m diameter area 105 m^2	Research and heating 185 m^2 house	$5,700 Liner - $1,500 Salt - $1,400 + equipment, labor and construction
Tennessee Valley Authority	Spring 1982	4000 m^2 3 m deep	Research, 140 KWt Energy Extraction	$1,640,000 (Refer to Table 4.4 for details)
Wooster, Ohio	1975	18.3 m x 8.5 m x 3 m	For heating a greenhouse	
Alice Springs, Australia		2000 m^2 > 2 m deep	Research	Not available

Table 1.1 Continued

PROPOSED PONDS

LOCATION	DATE COMPLETED	DIMENSION	PURPOSE	COST (installation)
Salton Sea, California		1 km^2 5 m deep	5 MWe Demonstration pond	$\$25*10^6$ - $30*10^6$
Salton Sea, California		12 modules (50 MWe each) 106 km^2	Energy generation 600 MWe + salinity reduction of lake	$\$1.1*10^9$
Truscott Brine Lake, Texas		80000 m^2	To supply energy for Red River chloride control project 1.9 MWe at 15% plant capacity factor	$\$5*10^6$
New Dead Sea Pond I		10 acre	5 MWe peaking (few hours/week) Research	
New Dead Sea Pond II	Fall 1982	60 acre	5 MWe peaking Research	

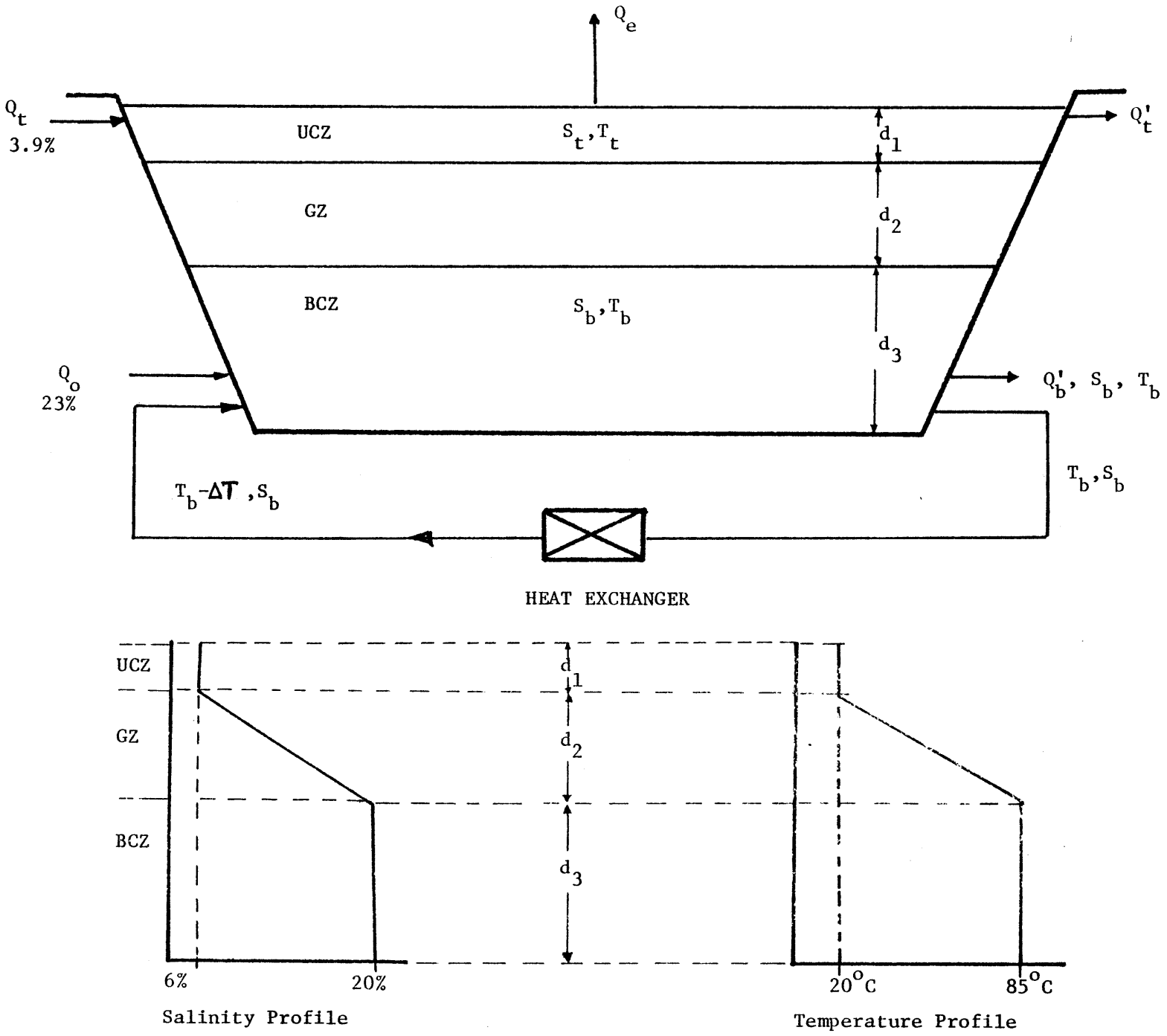

Figure 1.1 Structure, Salinity and Temperature Profiles for a Typical Solar Pond

is typically 0.3 to 0.5 m deep. It consists of uniform, relatively low salinity water (0 - 6 %) and temperature that is in equilibrium with the ambient meteorology. Below this is the stagnant gradient zone (GZ) where both temperature and salinity increase with depth. This zone varies from 0.75 m to 1.5 m in thickness. The bottom convecting zone (BCZ), usually about 1.0 m to 1.5 m thick, is the thermal storage zone with salinity reaching saturation levels. Solar energy penetrating this zone raises its temperature. The high density of this zone due to salinity suppresses thermal convection, thus enabling its temperature to reach values of $40^{\circ}C$ - $50^{\circ}C$ above that of the upper convecting zone. Figure 1.2a and Figure 1.2b show temperature and salinity profiles for the Argonne National Laboratory pond and the Miamisburg, Ohio ponds listed in Table 1.1. A record temperature of $107.2^{\circ}C$ was reached in an experimental pond at the University of New Mexico when the concentrated brine boiled causing the pond to mix. This high temperature was caused by the lack of withdrawal of heat form the bottom convecting zone. The effectiveness of a solar pond as an energy collector and storage device depends on a number of factors some of which are discussed below.

Solar Energy Penetration and Absorption

Depending on the nature of radiation (diffuse or direct), refractive index of water, the concentration of suspended substance, and the angular position of the sun, a portion of the solar energy impinging on the water surface is reflected. This is generally assumed to be between 6 and 10% of the incoming solar radiation (4). The remaining radiation penetrates the surface and is attenuated by absorption and scattering. This attenua-

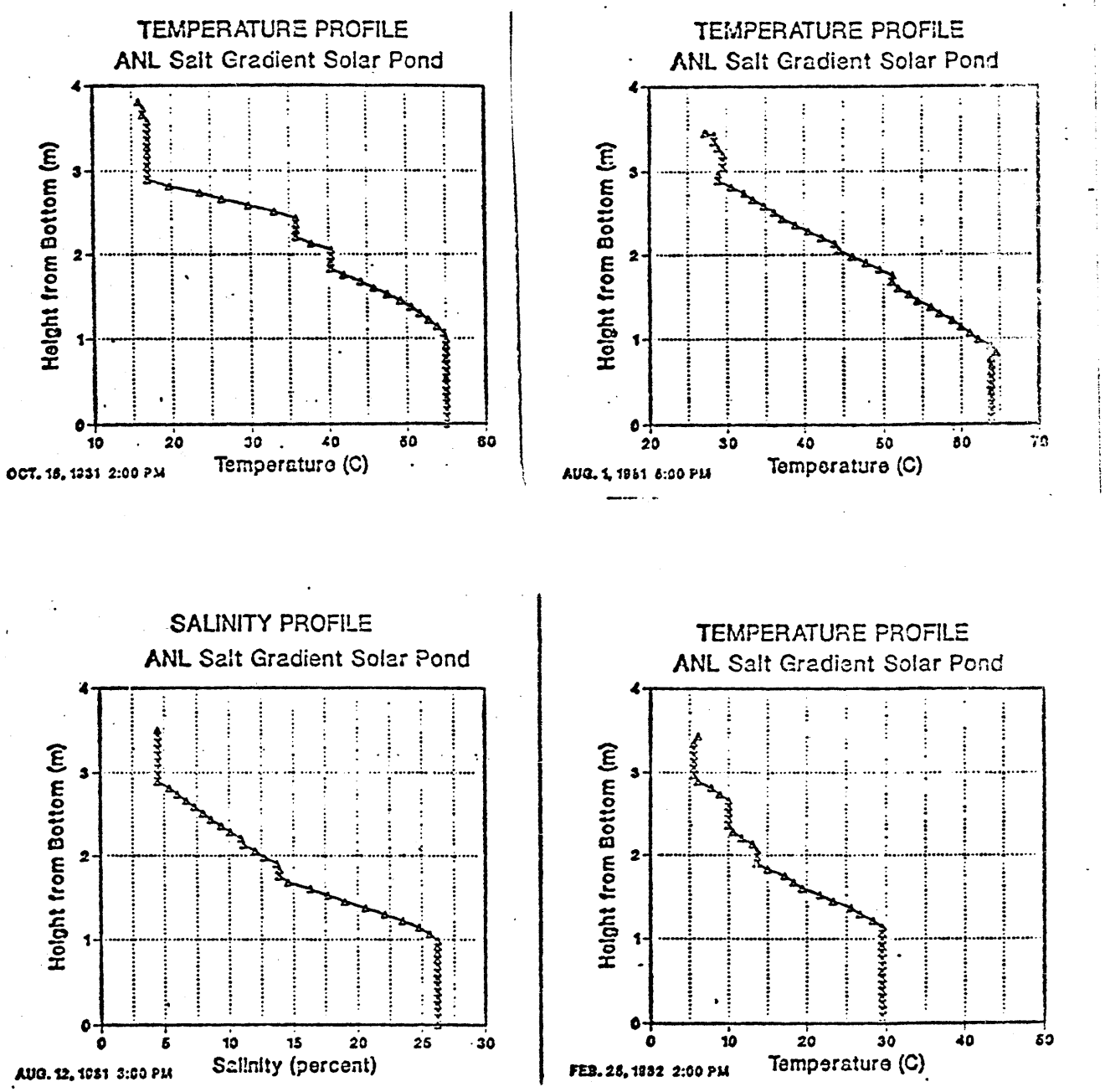

Figure 1.2a Temperature and Salinity Profiles for Research Pond at Argonne National Laboratory, Illinois. (2)

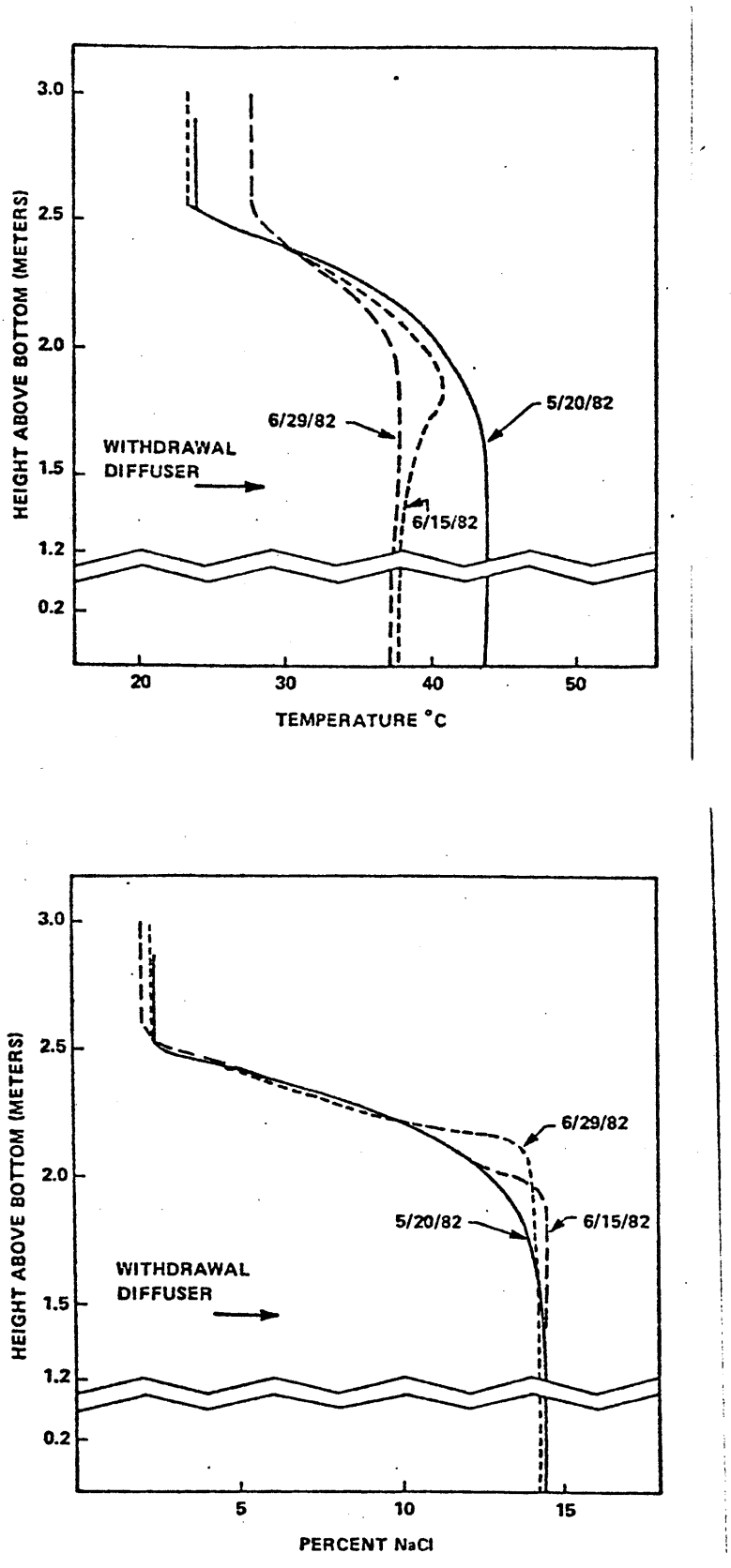

Figure 1.2b Temperature and Salinity Profile for 2000 m^2 Pond at Miamisburg, Ohio, with Heat Extraction. (3)

tion is a complex function of the wavelength and the clarity of water. In particular, the infra red component constituting about half of the solar energy spectrum is absorbed in the first few centimeters. Figure 1.3 compares the transparency of five different types of waters for solar radiation. Depending on the optical properties of water and the depth of the BCZ; typically 20% to 40% of the incoming solar radiation penetrates to the lower storage zone.

Several models have been proposed to predict the attenuation of solar energy with depth. A two parameter exponential decay model commonly used is (6)

$$\phi_s(z) = 0.94\ (1-\beta)\phi_o\ \exp(-\eta z) \qquad 1.1$$

where $\phi_s(z)$ = energy (W/m^2) reaching a depth z(m) below the water surface, β = the fraction of incoming solar radiation absorbed at the surface, ϕ_o = the total incoming solar radiation (W/m^2), η = extinction coefficient (m^{-1}) and the fraction 0.94 refers to the fraction of ϕ_o heat that is not reflected at the surface. For unpolluted natural water bodies typical values of η and β are 0.5. More accurate values for a pond can be determined by taking secchi disk measurements or by using submersible pyranometers (7). Other models that divide the solar spectrum into N parts and require 2N parameters have been proposed. Rabl and Nielson (8) have used models with N = 4 and Hull (9) has used a model with N = 40.

Fallen leaves, dust and debris can considerably reduce the transparency of the pond. These have to be removed from time to time either by surface flushing or other cleaning techniques. After a severe dust storm, the entire surface layer may have to be pumped and filtered (10).

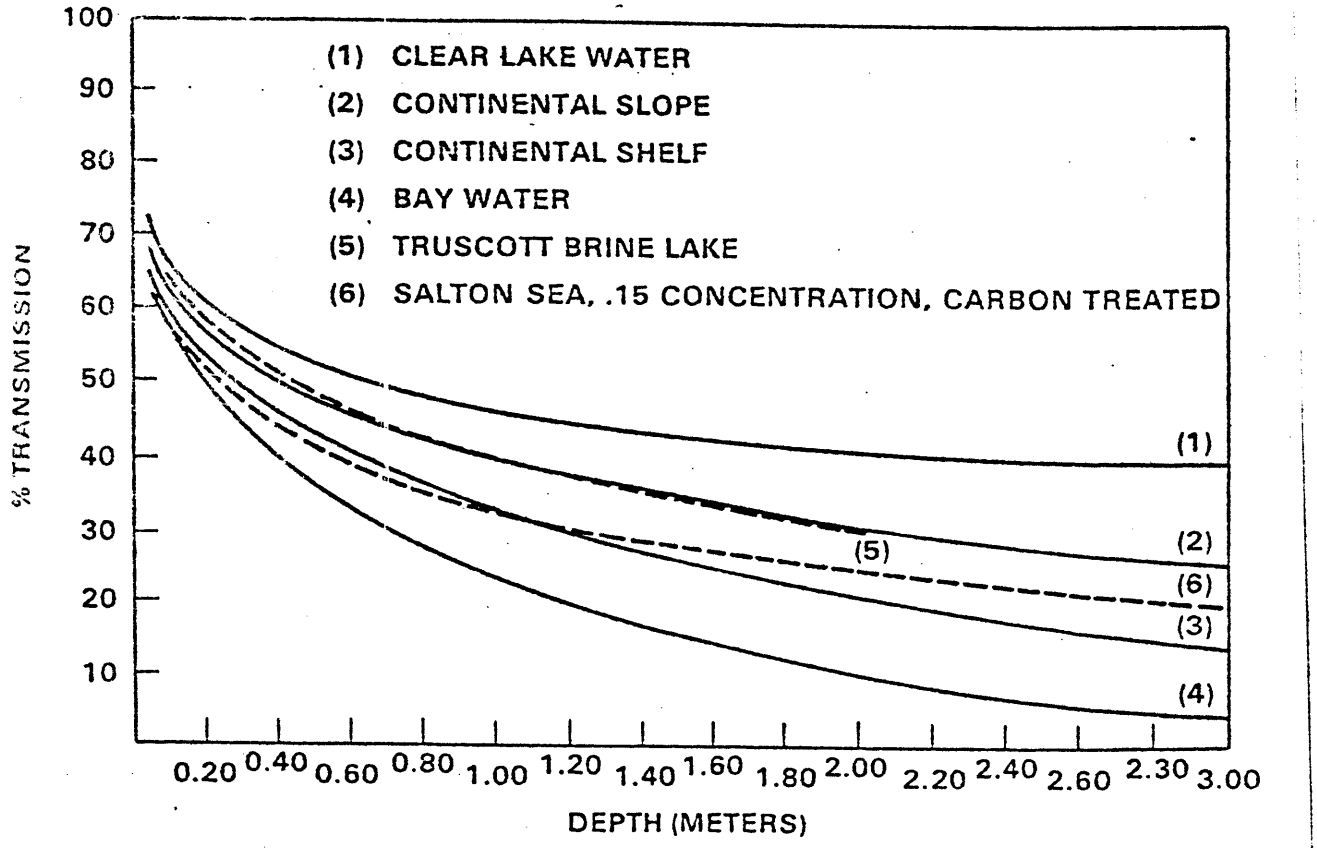

Figure 1.3 Comparison of Transparency of Five Different Saline Water Bodies. (5)

Turbidity caused by thermophylic and halophylic algae can be treated using copper sulphate or other chemicals.

Energy Budget for Solar Ponds

Figure 1.4 gives a diagrammatic heat balance for a typical solar pond. Figure 1.5 is an energy balance for a proposed 50 MWe (module) pond on the Salton Sea, California. With an UCZ of 0.5 m, a GZ of 1.0 m, $\eta = 0.5\ m^{-1}$ and $\beta = 0.5$, 22% of the incoming solar energy penetrates into the BCZ causing its temperature to rise. Heat losses occur by conduction through the boundaries of the BCZ and upwards through the GZ. For large ponds heat loss from the sides is negligible; that through the GZ is small (but not negligible) due to the low thermal conductivity of water and the large depth of the GZ. Losses through the bottom of the pond are highly site specific depending on the thermal conductivity of the soil and the depth to the water table. The effect of pond size, shape and various insulation strategies has been studied by Hull et al. (13). A high water table ($\leq$ 4 m) with a flowing aquifer can convect a large percentage of the energy trapped. For example, an increase in the thermal conductivity of soil from 1 W/m^oC to 5 W/m^oC results in a reduction in pond output of 40% (5). In the absence of a high water table heat loss to the ground is significant during the first year of pond operation after which the ground approaches a steady state. During succeeding years it acts as an additional storage unit to increase the thermal inertia of the pond. Figure 1.6a and Figure 1.6b show the temperature profiles within and below two operating ponds. The profiles were measured with a network of thermocouples buried under the pond.

Energy losses can also occur by leakage of hot brine. Excessive

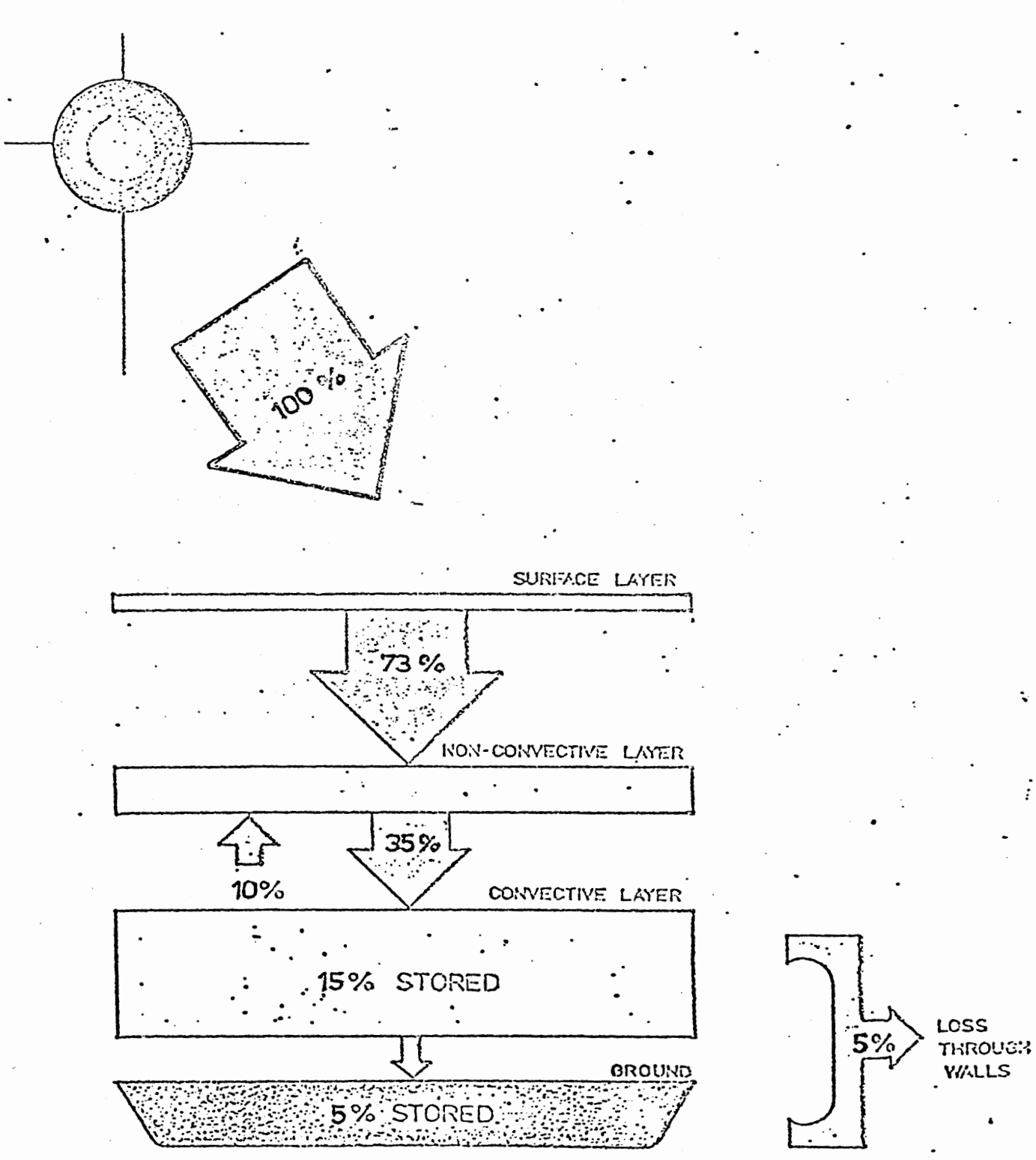

Figure 1.4 Diagrammatic Heat Balance for a Typical Pond. (11)

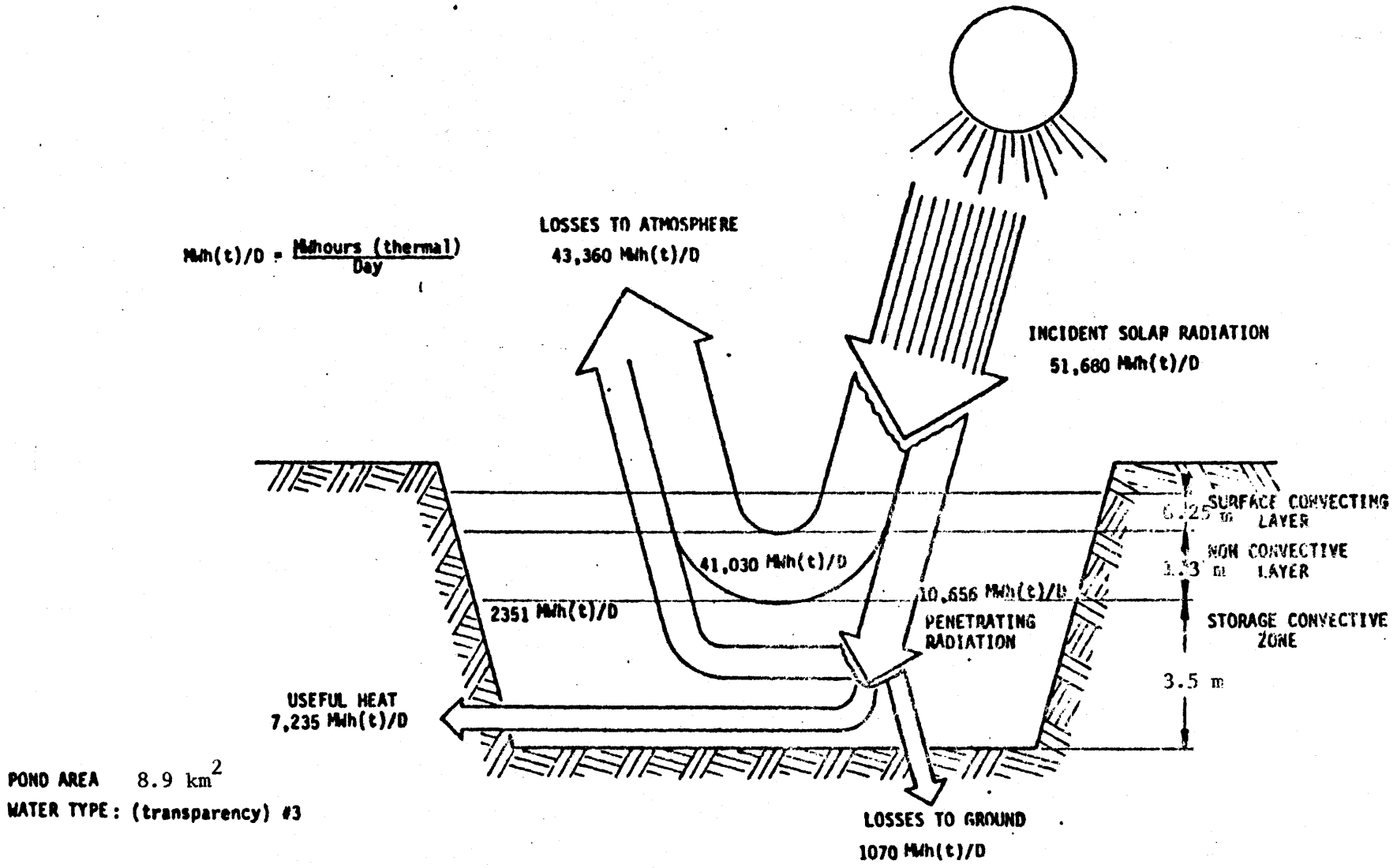

Figure 1.5 Energy Balance for a 50 MWe Solar Pond Proposed for the Salton Sea, California (12)

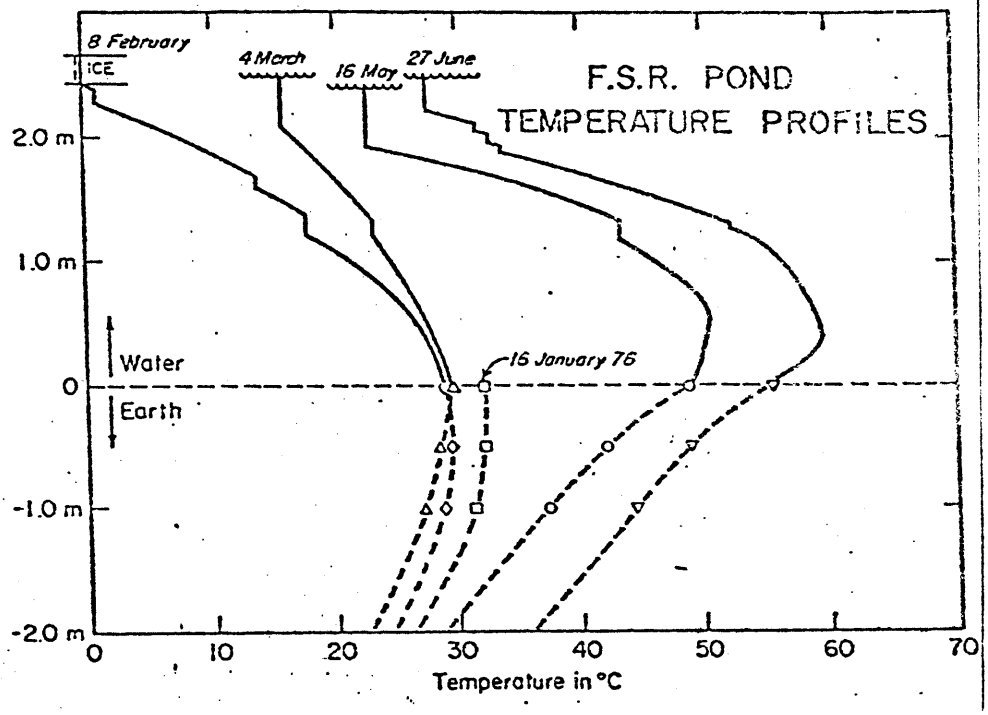

Figure 1.6a Temperature Profiles Within and Below the Circular Pond at New Mexico University. (11)

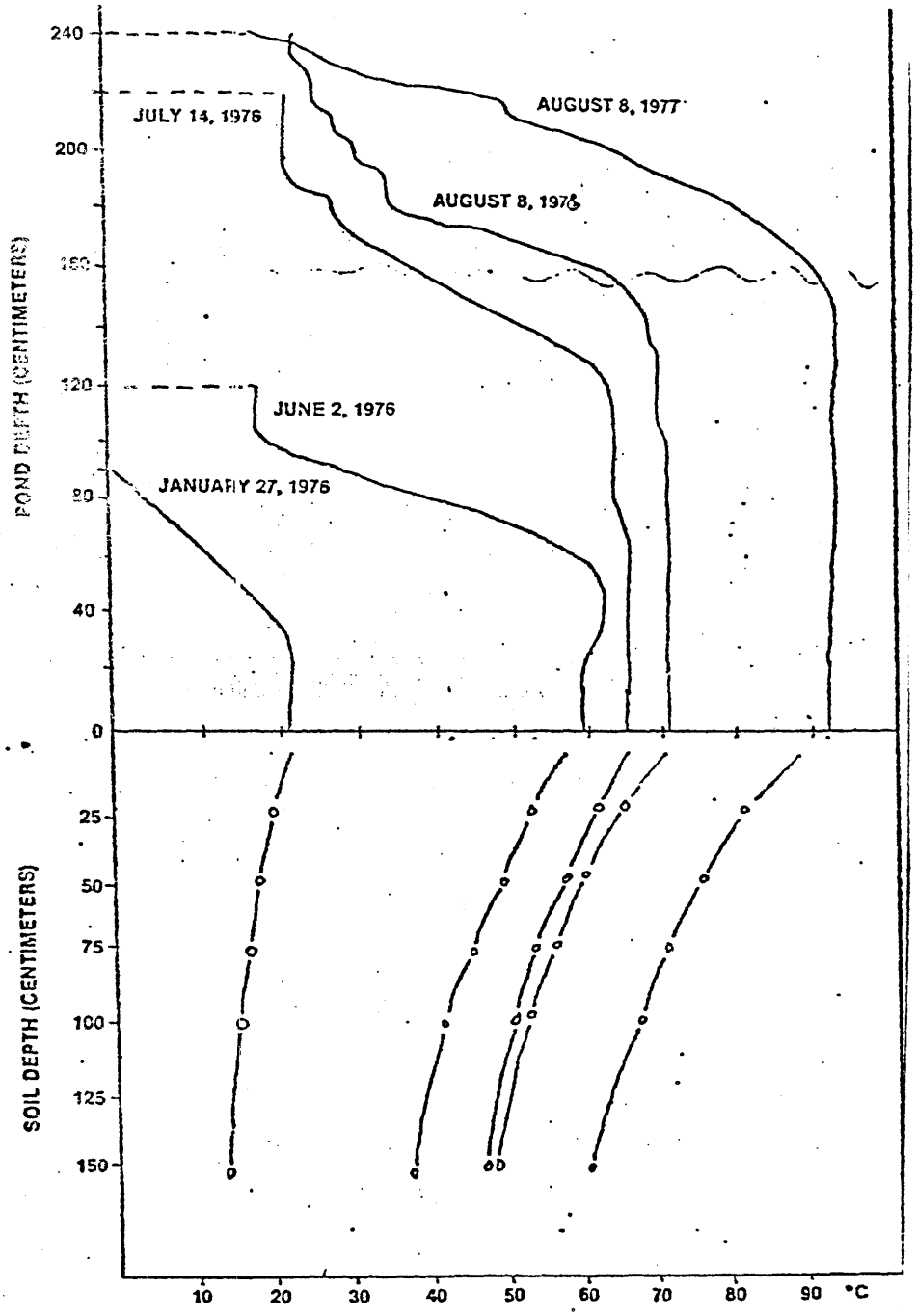

Figure 1.6b Temperature Profiles Within and Below 200 m^2 Ohio State University Pond. (14)

leakage can make the entire project uneconomical. To date most experimental ponds have been lined. However, for large ponds this would considerably reduce the benefit to cost ratio. In addition to heat loss, leakage can contaminate regional aquifers.

Energy Extraction

Two methods have been used for energy extraction. For small ponds a heat exchanger consisting of a set of closely spaced copper tubes can be placed in the BCZ (14). This method is infeasible for large commercial ponds. The best available options is to extract hot brine from one end of the pond using a manifold, pass it through an external heat exchanger and return the cooled brine to the BCZ at the other end of the pond.

For the generation of electricity, heat from the brine would be used to evaporate an organic working fluid such as freon or ammonia. Ideally the brine is extracted at about $80^{o}C$ and returned to the pond after a $5^{o}C$ drop. The working fluid drives a Rankine cycle turbine to generate power. Presently, Ormat Turbine Ltd., Israel, is marketing such turbines in the KW range (Ref. 1 and personal communication). Research is being conducted in Israel and elsewhere to construct larger units. The 7000 m^2 pond at Ein Bokek, Israel, uses an organic turbogenerator for 150 KWe of peaking power.

Figure 1.7 shows a schematic diagram of heat extraction and power generation from a solar pond. An evaporation pond which is a necessary supplement to a solar pond, unless an existing saturated brine source is available, can be used as a sink for waste heat rather than the UCZ as shown in Figure 1.7.

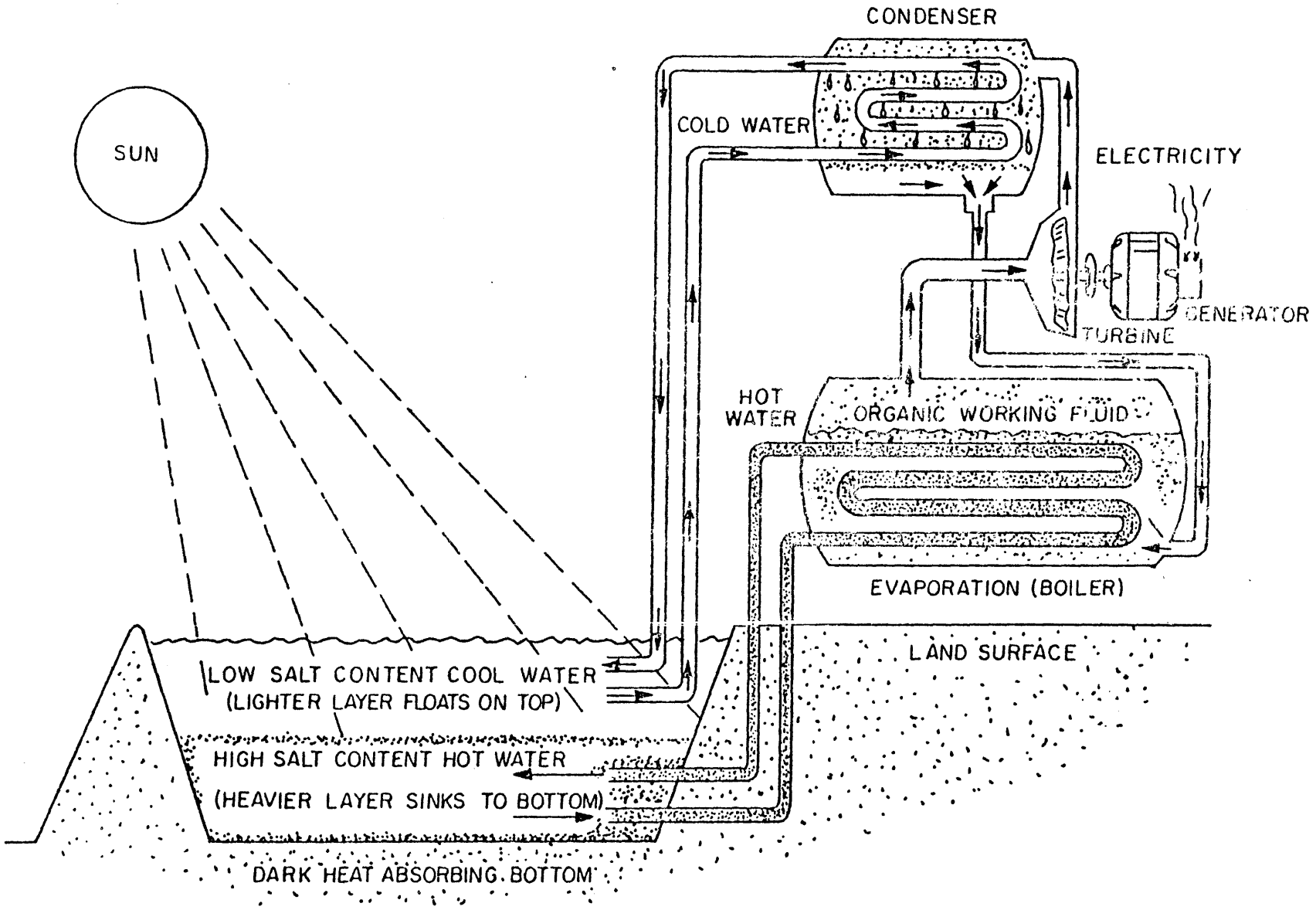

Fig. 1.7 Schematic Diagram of Heat Extraction and Power Generation from a Solar Pond

The energy extracted from solar ponds can be used for a variety of other purposes such as desalinization, space heating, industrial process heat, etc. An extensive study conducted by the Jet Propulsion Laboratory at the California Institute of Technology details the economics of various schemes of energy utilization for different regions in United States (15). A 2000 m^2 pond--the largest presently in operation for energy production in the USA--uses the extracted energy to heat a public swimming pool in summer (3).

One of the major advantages of solar ponds over other solar collectors is their large thermal inertia and storage capacity. This enables the BCZ to maintain a fairly uniform temperature over a 24-hour period despite the diurnal variations in the incoming solar energy. Figure 1.8 shows the daily temperature response of the circular experimental pond at New Mexico University.

The thermal inertia of a solar pond over longer time scales was demonstrated by further experiments conducted at New Mexico State University. The 2.5 m deep circular pond was covered with sheets of black polyethylene for eight days to completely cut off all incoming solar radiation (16). The BCZ temperature dropped from 86°C to 75°C linearly at a rate of 1.4°C/day.

The effect of seasonal variation in insolation and ambient air temperature on the heat storage in the BCZ is shown in Figure 1.9. Two or three months of snow and ice coverage on the surface did not degrade the solar pond. Ponds located in low insolation, northern latitudes are capable of sustaining a temperature of about 30°C in BCZ even when the surface is frozen (Figure 1.6a).

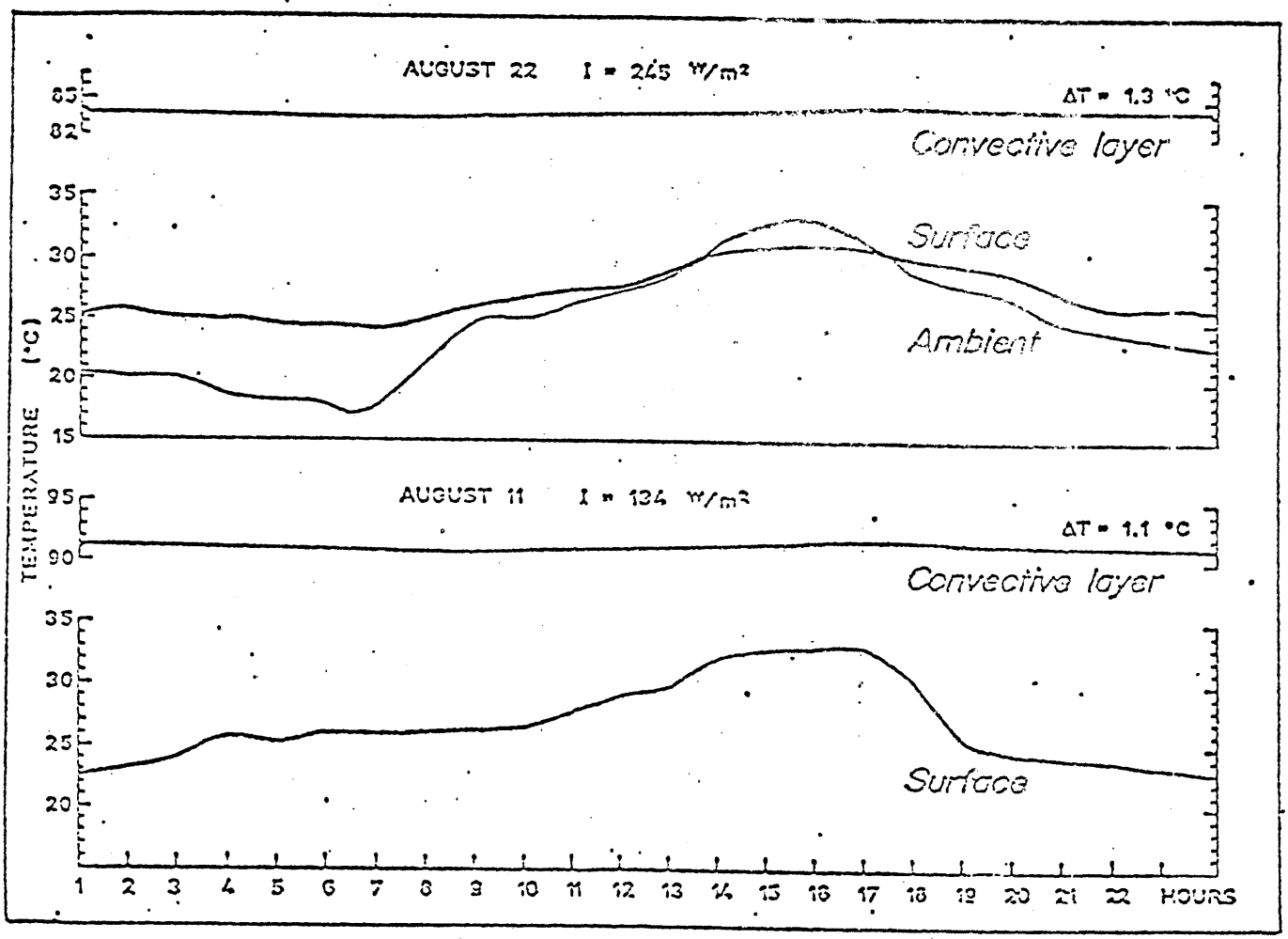

Figure 1.8 Daily Temperature Response of the Circular Pond at New Mexico University. (11)

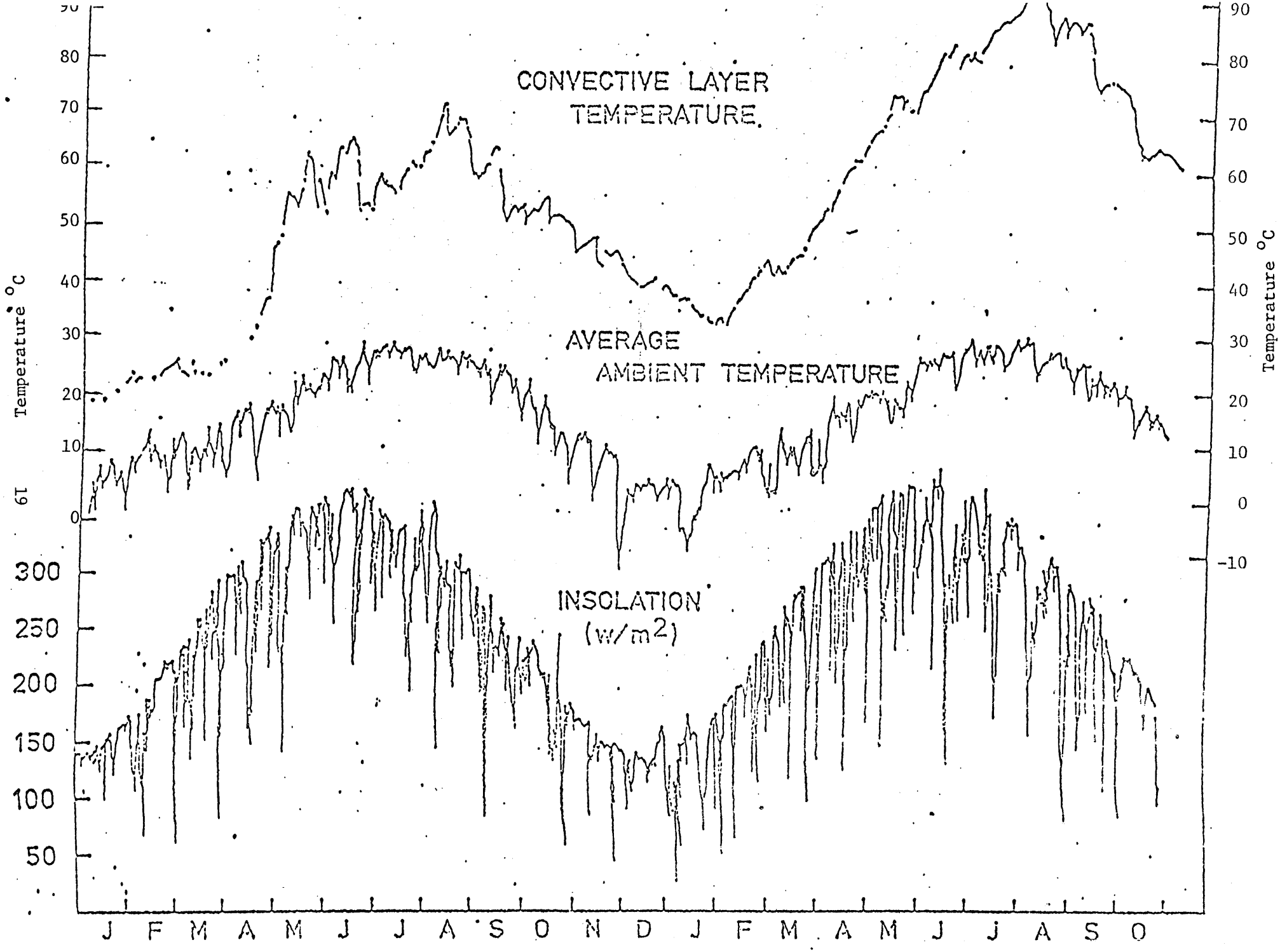

Figure 1.9 Seasonal Variation in Temperature of the Circular Pond at New Mexico University. (11)

Construction and Maintenance of the Pond

The initial filling of the pond involves establishing the three zones and the design gradient. A number of methods have been proposed (17). The pond can be filled in layers, 5-10 cms thick with successively lesser salinity, starting with the BCZ. Alternately, the less dense UCZ is first placed in the pond and progressively denser brines injected from below. In both these methods, the initial step structure rapidly smooths out due to molecular diffusion.

Zangrando (18) has proposed a simple method using a horizontal diffuser to establish a linear gradient. With this method, the entire operation can be performed manually or automatically, continuously or intermittently. This method was used to fill the Miamisburg Pond in Ohio. Having established the linear gradient up to the surface, redistribution of salt takes place in the top 20-30 cms to form the UCZ.

Excessive growth of the UCZ is detrimental to the efficiency of a solar pond as it results in increased heat losses through the GZ. Models have been developed to predict the growth of the UCZ and the sensitivity of the pond efficiency to the depth of the UCZ. For small ponds these results have been well reported. However, some uncertainty exists in scaling results from small ponds to larger, commercially feasible ponds in which wind and wave mixing would be more severe. Figure 1.10 (19) shows the growth of the UCZ for a 3 m deep large hypothetical pond as predicted by the model developed at MIT. In Israeli ponds, floating plastic grids are being used to reduce mixing due to winds and waves. As yet sufficient data is not available to assess their effectiveness.

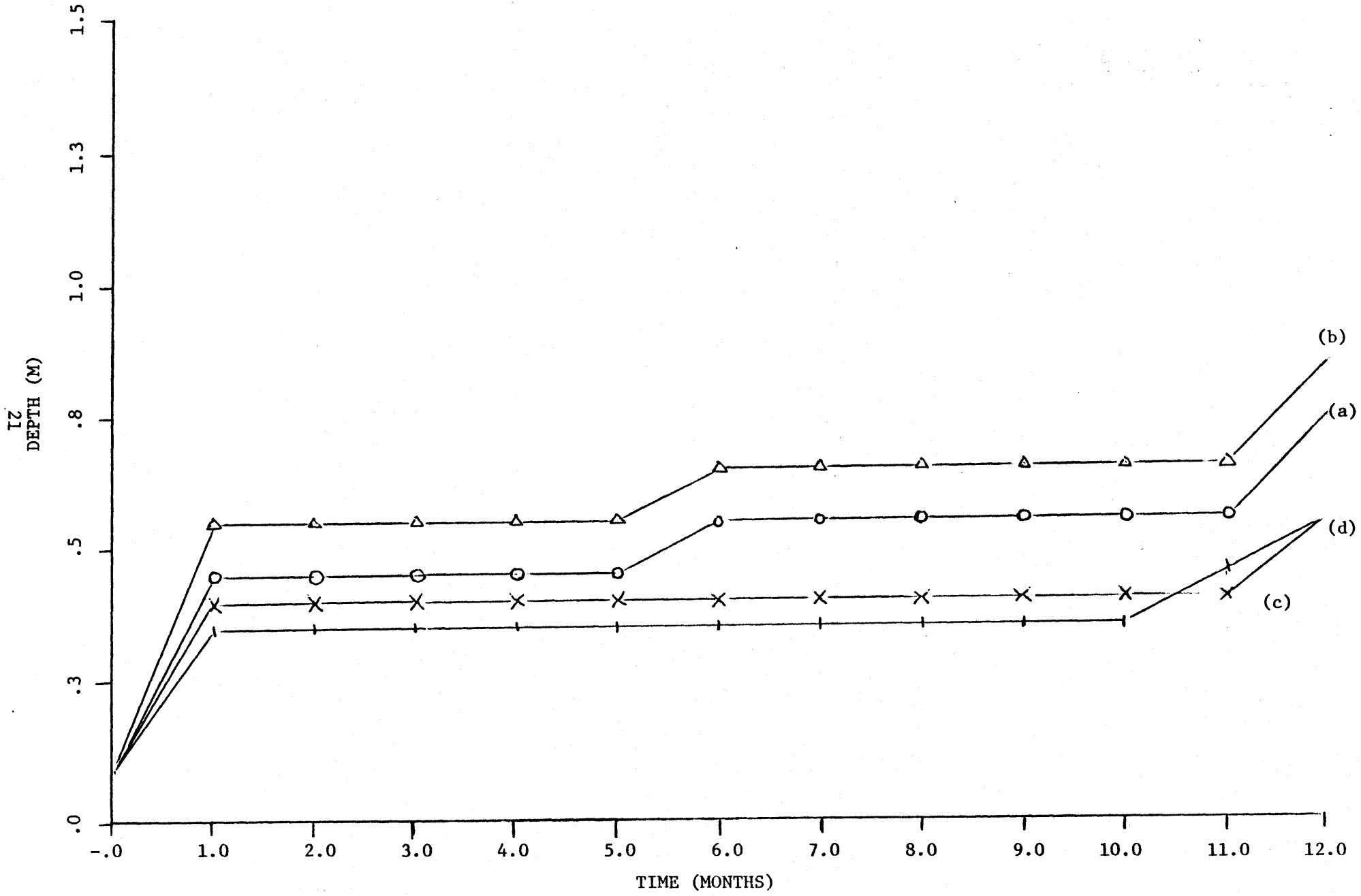

Figure 1.10 Growth of the Upper Convective Zone for a 3 m Deep Large Hypothetical Pond--Model Results (14)

The maintenance of the three zones is achieved by continuous or intermittent flushing of the UCZ with freshwater. This counteracts the concentration effects of evaporation and the upward diffusion of salt. In addition, the BCZ has to be concentrated to compensate for the salt lost by diffusion. Water flushed from the UCZ is concentrated in an adjacent evaporation pond to produce saturated brine for concentrating the BCZ. Figure 1.11 gives a schematic diagram of the brine flows for the 5 MWe demonstration plant proposed for the Salton Sea.

Resources Required

The technical and economic viability of solar ponds critically depends on the availability of four resources--insolation, land, salt and water. Each of these is discussed below.

Insolation This is a key parameter that affects the operation of a solar pond and to a large extent determines the amount of energy that can be extracted as well as its seasonal variation. Since regions with high solar insolation are preferred it implies that best locations for solar ponds are at lower latitudes and in regions of low cloud cover. No lower threshold value for insolation has been defined, but most ponds in operation are in areas with annual average insolation levels of over 200 watts/m^2.

Land The density of electric energy that can be obtained from solar ponds varies from 3-5 MW/km^2. As such, large land areas are required to construct ponds. These areas should be flat, horizontal, impermeable and relatively inexpensive. The land cost can be reduced by

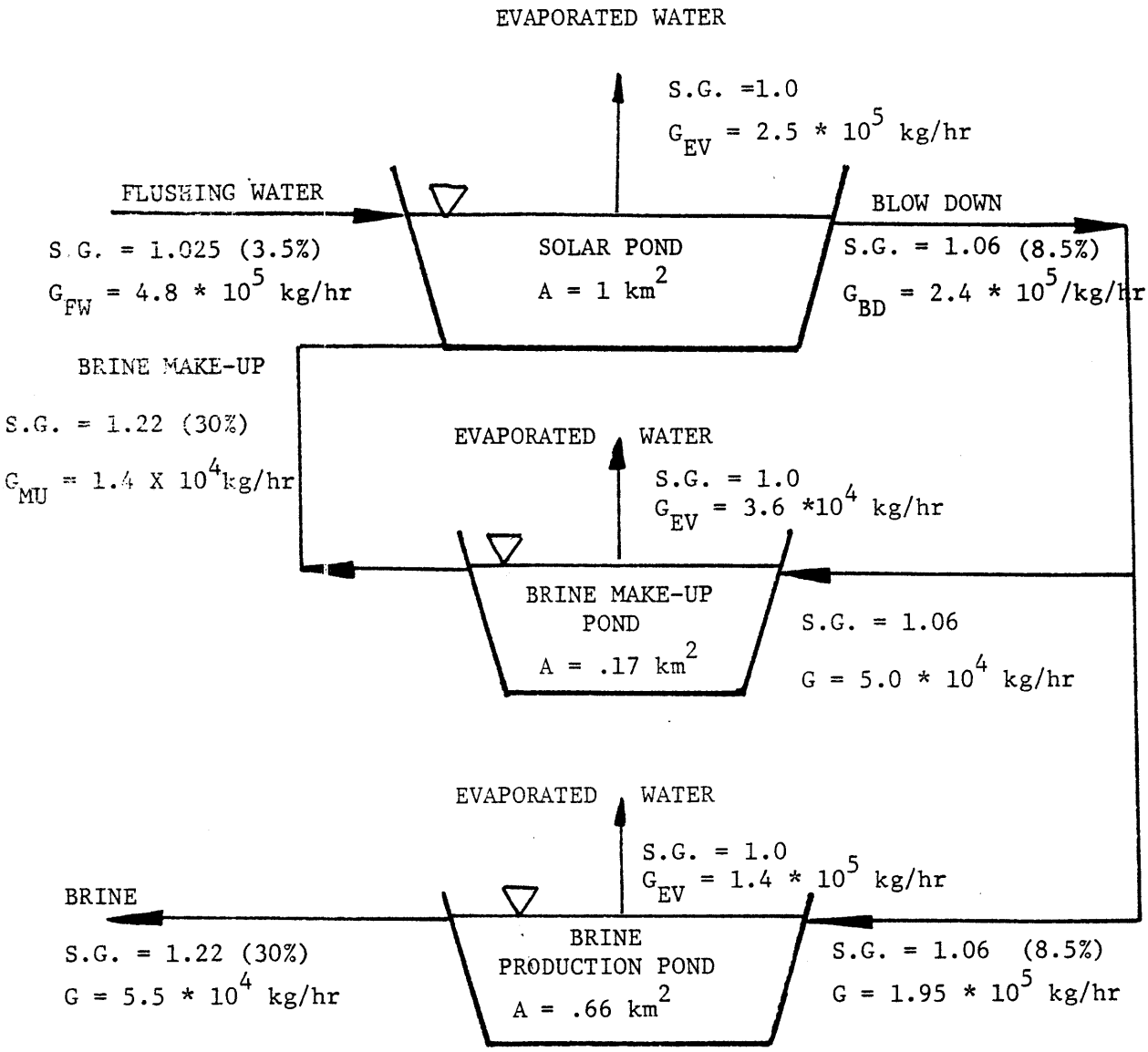

LEGAND

SG - SPECIFIC GRAVITY
G_{FW}- FLUSHING WATER RATE
G_{BD}- BLOW DOWN RATE
G_{MU}-MAKEUP BRINE RATE
G_{EV}-EVAPORATION RATE
G -BRINE MASS FLOW

Figure 1.11 Schematic Diagram of Brine and Water Flows for the Proposed 5 MWe Salton Sea Solar Pond (12)

building ponds in existing shallow lakes. Land availability and land value vary from site to site and affect the economics of solar ponds.

Salt The availability of abundant supplies of salt, brine or sea water in the proximity of a solar pond site is very important. A 3 m deep pond with 1.5 m deep SCZ requires over 50 tons salt/100 m^2 of area. For small experimental ponds salt can be purchased, but for large ponds in situ availability of salt is required. Ocean water or irrigation return flow may be concentrated by evaporation to produce enough brine to start a pond as proposed for the Salton Sea Solar Ponds and at Lake Truscott (12,5). This has the added advantage of arresting and possibly decreasing the salinity of the existing water body.

Water Fresh water or low salinity water, such as sea water, is required for the UCZ and the gradient zone at the initial filling of the pond. Once the pond is in operation make up water for evaporation as well as for flushing the UCZ to counteract the effect of molecular diffusion is required. Evaporation takes up to 2 m of water per year in some regions. Saline water with low salinity, e.g., sea water or agricultural return flow, can also be used for this purpose.

Cost of Energy from Solar Pond Systems

The cost of energy extracted from solar ponds depends on a number of site-specific factors such as the level of insolation, value of land and its characteristics, the necessity of lining, the availability of salt or saturated brine and a continuous supply of fresh or brackish water.

In addition, the cost is also a function of pond size, its performance and its purpose--whether for thermal or electric energy extraction or for research and development. Owing to these reasons, widely differing estimates have been quoted in the literature. Table 1.2 lists the cost of energy from solar ponds as estimated by Tabor (1). A large variation in cost from 5.3¢/KWh to 13.5¢/KWh is indicated. More recent estimates for conditions prevailing in the US are given in Tables 1.3a-1.3c (20) For thermal energy applications the cost of liner, salt ($10.00 per ton) and land ($1,000/acre) are included. For electric power applications, these costs are not included. These estimates also indicate the very variable and site specific nature of solar pond economics. Table 1.4 gives a breakdown of the expected cost of installing and maintaining a 5 MWe demonstration pond at the Salton Sea.

Optimization of the Solar Pond

The energy output from a solar pond depends on a number of parameters, with obvious trade-offs between some of these parameters. The construction, design, operation and maintenance present many optimization problems, the objectives of which are to determine the set of parameters which will minimize the cost of installed capacity /KW of power. Some of the important decision variables are the depths of UCZ, GZ, and the BCZ, extraction of energy--base load or peaking--and its conjunctive operation with other regional power sources, the sizing and location of pond, pumps and piping, etc. Optimization studies for the 600 MWe facility at Salton Sea have indicated the merits of a modular

Table 1.2 Estimated Power Costs for SPPS* in Sunny Climate (1)

(Solar Input 2000 KWh/m^2-yr. 1 km^2 pond area)

	Lined Pond	Unlined Pond
Construction Cost	$13/$m^2$	$8/$m^2$
Capital Power Plant Cost[1] $/KW	$1500	$1500
	Annual Costs[2]	
Pond	1,521,000	913,000
Water	200,000	200,000
Maintenance	100,000	100,000
Power Plant	877,500	877,500
Total	2,698,500	2,090,000
	Bus-Bar Power Costs[3]	
Cents/KWh[4]	8.1	5.9

* SPPS Solar Pond Power Station

(1) Plant refers to turbogenerators, heat exchangers and all auxilliaries: 5MWe installed.

(2) Annual Costs at 11.7% annual charges on capital and 15 years lifetime.

(3) Excludes station operating costs.

(4) At 20% collection efficiency and 8% thermodynamic conversion efficiency.

Table 1.3a Estimated Cost of Construction of Large Solar Pond Systems[20] ($/m^2 of pond area)

Application	Best Case	Conservative Case
Thermal Energy @75°C	7	28
Electricity baseload	12	20

Best Case: excludes salt, land and liner costs and assumes availability of advanced technology and equipment

Conservative Case for thermal energy includes cost of land and liner and salt.

Electric power applications: land, liner and salt costs are excluded.

Table 1.3b Estimated Performance of Solar Pond System[20]
(KW/km^2 of pond area)

Application	Average Site	Superior Site
Thermal Energy at 75°C	29	54
Electricity Baseload	2	3.5

Average Site: mean annual Solar Radiation 215 W/m^2
mean annual air temperature 17°C

Superior Site: mean annual solar radiation 270 W/m^2
mean annual air temperature 23°C.

Table 1.3c Estimated Cost of Energy [20]

(using 20% Annual Fixed Charge Rate and figures from Tables 1.3a and 1.3b)

Case	Thermal/Energy ¢/KWh	Electricity ¢/KWh
Conservative Construction cost, average site	2.2	26
Conservative Construction cost, Superior site	1.2	13
Best Case Construction cost, average site	0.6	16
Best Case, Construction cost, superior site	0.3	8

COST ACCOUNT NO.	ITEM	COST (1,000 $)	
		1st. DEMONSTRATION SPPP	2nd. ADJACENT SPPP
100	Solar Pond Systems		
101	Geotechnical Survey	220	120
102	Solar Pond Construction	6,765* - 7,500**	6,765 - 7,500
103	Construction of Evaporation Ponds	2,206* - 5,206**	-
104	Brine Circulation System	752	600
105	Cooling System	510	400
106	Water Flushing System	140	120
107	Water Treatment Plant	1,000	800
108	Gradient Control System	650	650
109	Instrumentation and Controls	72	50
110	Power Station Yard Development	128	128
111	Engineering and Design	995 - 1,294	300 - 450
112	Management, Supervision & Administration	500 - 600	300 - 400
	Sub Total	13,938 - 18,072	10,233 - 11,218
200	Power Generating Unit		
201	Plant Equipment	4,650	4,200
202	Construction Materials	1,550	1,550
203	Construction and Installation	800	630
204	Engineering and Design	700	150
205	Management, Supervision & Administration	400	150
	Sub Total	8,100	6,680
	TOTAL	22,038 - 26,172	16,913 - 17,898
	Contingencies (15%)	3,306 - 3,926	2,537 - 2,685
	GRAND TOTAL	25,344 - 30,098	19,450 - 20,583
	O & M Costs - 3 Years	1,541	353

* Borrow material within Sea

** Borrow material available on shore

Table 1.4 Estimated Cost of a 5 MWe Demonstration Pond at Salton Sea, California (12) Area = $1km^2$

approach, with each unit ranging in size from 20 MWe to 50 MWe depending on the site conditions.

Given the right conditions, the potential of solar ponds for large scale power generation is very promising. Chapter 3 and Chapter 4 present a preliminary feasibility study for a large scale solar pond system in Egypt. Chapter 2 is a brief outline of solar pond research in the Ralph M. Parsons Laboratory for Hydrodyanmics and Water Resources (Department of Civil Engineering) at M.I.T.

2. Solar Pond Research at MIT

Introduction

Solar pond research in the Ralph M. Parsons Laboratory for Water Resources and Hydrodynamics can be divided into two categories: first, the development of a numerical model to predict solar pond performance and second, experimental work to study the effect of wind mixing in double-diffusive systems in general and solar ponds in particular. The following section gives a brief review of these two activities.

The Numerical Model

The solar pond numerical model is the result of continuous research, development and improvements at MIT over a period of several years. It uses an explicit finite difference scheme to solve the differential equations governing the distribution of heat and salt in the vertical direction. These equations assuming horizontal homogeneity are:

$$\frac{\partial T}{\partial t} + \frac{1}{A}\frac{\partial}{\partial z}(wAT) = \frac{1}{A}\frac{\partial}{\partial z}\left(Ak_T \frac{\partial T}{\partial z}\right) + \frac{q_i T_i - q_o T}{A} + \frac{1}{\rho C_p}\frac{\partial}{\partial z}(A\phi) \qquad (2.1)$$

$$\frac{\partial S}{\partial t} + \frac{1}{A}\frac{\partial}{\partial z}(wAS) = \frac{1}{A}\frac{\partial}{\partial z}\left(Ak_s \frac{\partial S}{\partial z}\right) + \frac{q_i S_i - q_o S}{A} \qquad (2.2)$$

where the symbols are defined in the list at the end of this chapter.

The pond is divided into a number of homogeneous horizontal layers of thickness Δz. The area of the layers can vary. Computations are performed for each time step, Δt, which is user specified such that the following inequality holds:

$$k_T \frac{\Delta t}{(\Delta z)^2} \leq 1/2 \qquad (2.3)$$

This restriction on Δt is necessary to avoid numerical instability.

The boundary conditions at the surface consist of heat fluxes due to evaporation, conduction, and absorption and emission of long and short wave radiation. In addition, precipitation and evaporation affect the surface salinity as:

$$k_s \frac{\partial \rho_s}{\partial z} = \left(\frac{\phi_e}{\rho_c l_v} - \psi\right)\rho_s \quad \text{at } z = z_s \tag{2.4}$$

At the bottom of the pond, salt and water fluxes are considered zero. Heat flux through the bottom is determined by choosing appropriate values for thermal conductivity for the pond bottom and the soil below it.

Penetration of solar energy into the pond is modelled using Eq. 1.1. An extinction coefficient 'η' and surface absorption coefficient 'β' have to be specified. Other models as proposed by Rabl and Nielson (8) and Hull (9) can be easily included in the model.

The water balance and surface heat transfer are computed by two separate subroutines. These subroutines allow the inclusion of numerous options--calculation of evaporation using different formulae, inclusion of inflows and outflows, effect of salinity on evaporation, etc.

A distinctive feature of the model is the option of using various wind mixing algorithms developed in this laboratory (21). The model includes options of no wind mixing, full wind mixing (Hurley-Octavio algorithm) and wind-mixing using Bloss and Harleman algorithm with or without internal shear. The full wind mixing algorithm equates the input of turbulent kinetic energy (TKE) by the wind to the increase in the potential energy (PE) of the pond due to mixing across the thermocline. The Bloss and Harleman algorithm is an improvement to this for it includes the transient and dissipative effects on the

turbulent entrainment process. The ratio of change in PE of the mixed layer to the change in TKE due to wind shear during a time interval 'Δt' is expressed as a function of the Richardson number (Ri):

$$\frac{\Delta(PE)}{\Delta(TKE)} = f(Ri) \tag{2.5}$$

where,

$$f(Ri) = 1 \qquad \text{(full wind mixing) Hurley-Octavio algorithm} \tag{2.6}$$

$$f(Ri) = 0.057\ Ri\ \left\{\frac{29.5-\sqrt{Ri}}{16.2+\ Ri}\right\} \qquad \text{Bloss and Harleman without internal shear} \tag{2.7}$$

$$f(Ri) = \frac{Ri}{14.2+Ri} \qquad \text{Bloss and Harleman with shear} \tag{2.8}$$

and

$$Ri = \frac{g\Delta\rho h}{\rho_o u_*^2}$$

Eq. 2.5 has been plotted in Figure 2.1. These algorithms have been discussed in detail in Reference 21.

At each time step, two stability conditions for the double diffusive system have to be satisfied. These are first, the density must increase with depth and second, the following inequality must hold:

$$\frac{\partial S}{\partial z} \geq -\left(\frac{\nu + k_T}{\nu + k_s}\right) \frac{\partial \rho}{\partial T} \frac{\partial T}{\partial z} \Big/ \frac{\partial \rho}{\partial S} \tag{2.9}$$

These conditions are checked at each iteration and adjacent layers mixed until the instability is eliminated. Any instability caused by surface cooling is also eliminated in a similar fashion.

The application of the wind-mixing algorithm and any mixing to eliminate surface instability results in a change in the surface temperature which in turn affects the surface heat transfer fluxes. An iter-

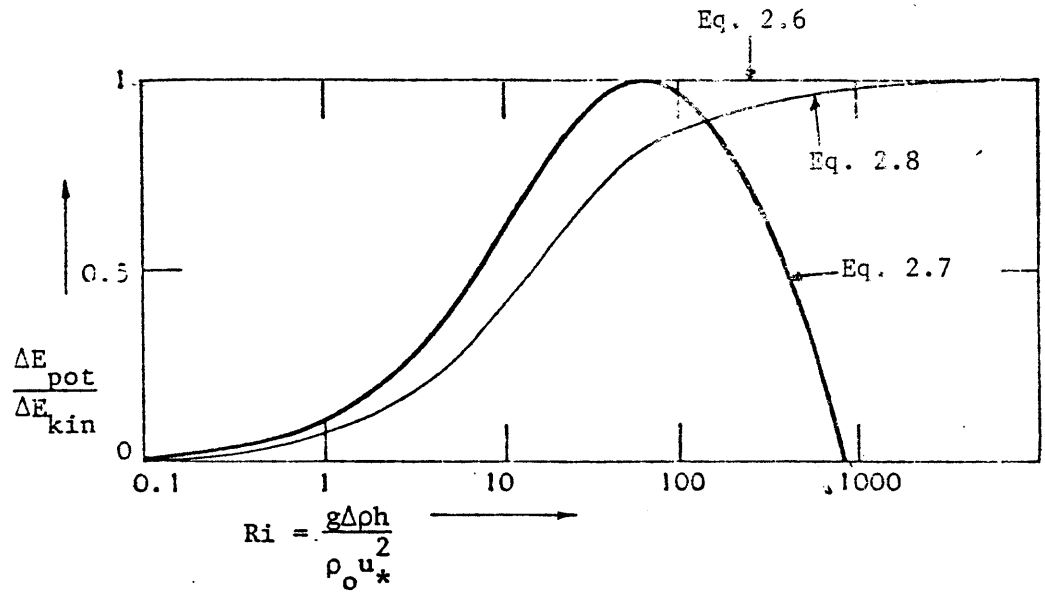

Fig. 2.1 Dependence of the Conversion of TKE into Potential Energy on the Richardson Number (21).

ative procedure is adopted, in each time step, in which the heating and mixing steps are successively applied until there is no significant change in the surface heat flux. The basic structure of the model is summarized in Figure 2.2. Further details are included in Reference 19.

Field Data from Solar Pond at Wooster, Ohio

To date the model has been tested with one set of field data from a 155 m^2, 3 m deep solar pond at Wooster, Ohio. Temperature and salinity profiles at 5 cm intervals were available along with the meteorological data--wind speed, solar radiation, precipitation, air temperature, humidity and cloud cover. Figure 2.3 is a comparison of the average storage zone temperature for the six month simulation period in 1980. The comparison is good except for the last few months when the predicted temperatures are somewhat higher than the measured. This is due to the fact that starting in October, energy was extracted from the pond and this is not included in the simulation due to inadequate data on the amount of energy extracted. Figure 2.4 is a comparison of the temperature and salinity proflies. These results have been discussed in greater detail in Reference 19 .

Efforts are continuing to further improve the model and to acquire more field data from other operating ponds to validate the model.

Small Experimental Solar Pond at MIT

In the summer of 1982 a small experimental solar pond was installed on the roof of this laboratory. The pond is circular with a diameter of 5.5 m and a depth of 1.0 m. The pond is insulated at the sides and the bottom. The initial filling of the pond was completed in July 1982.

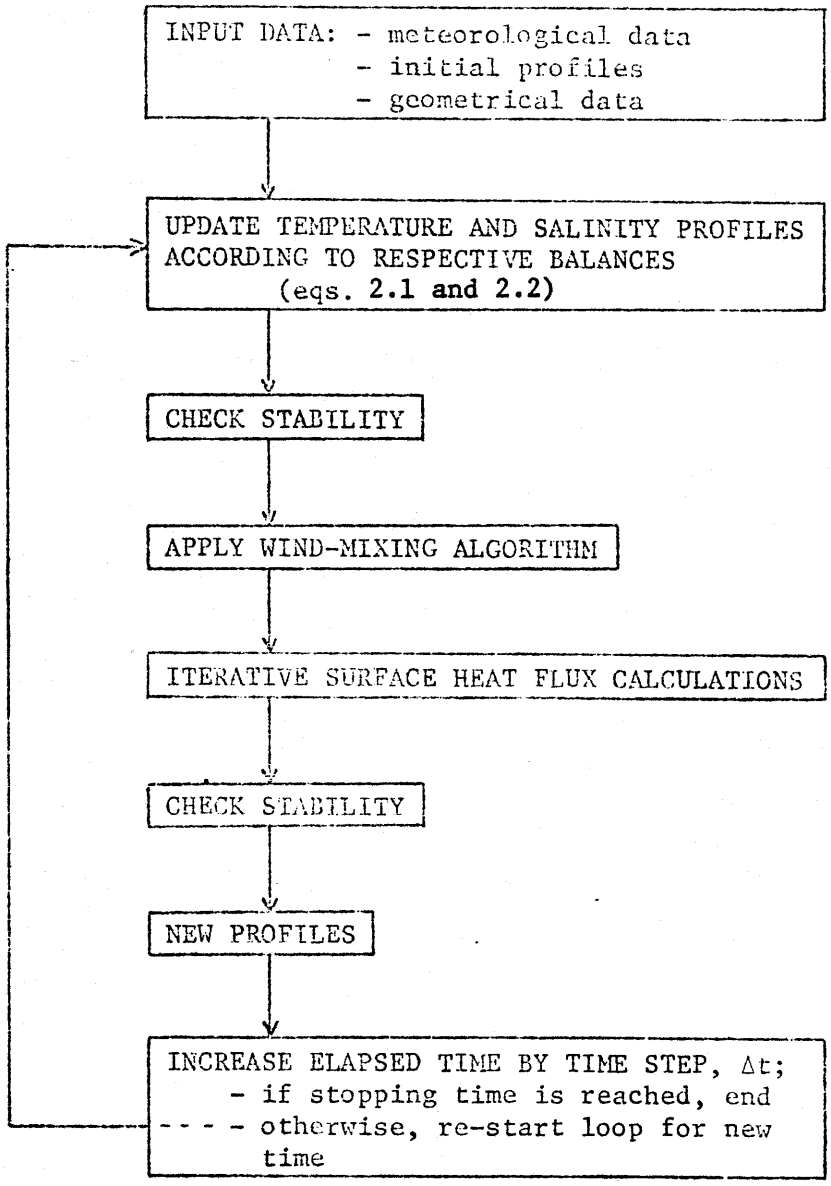

Fig. 2.2 Basic Structure of the Numerical Model (19).

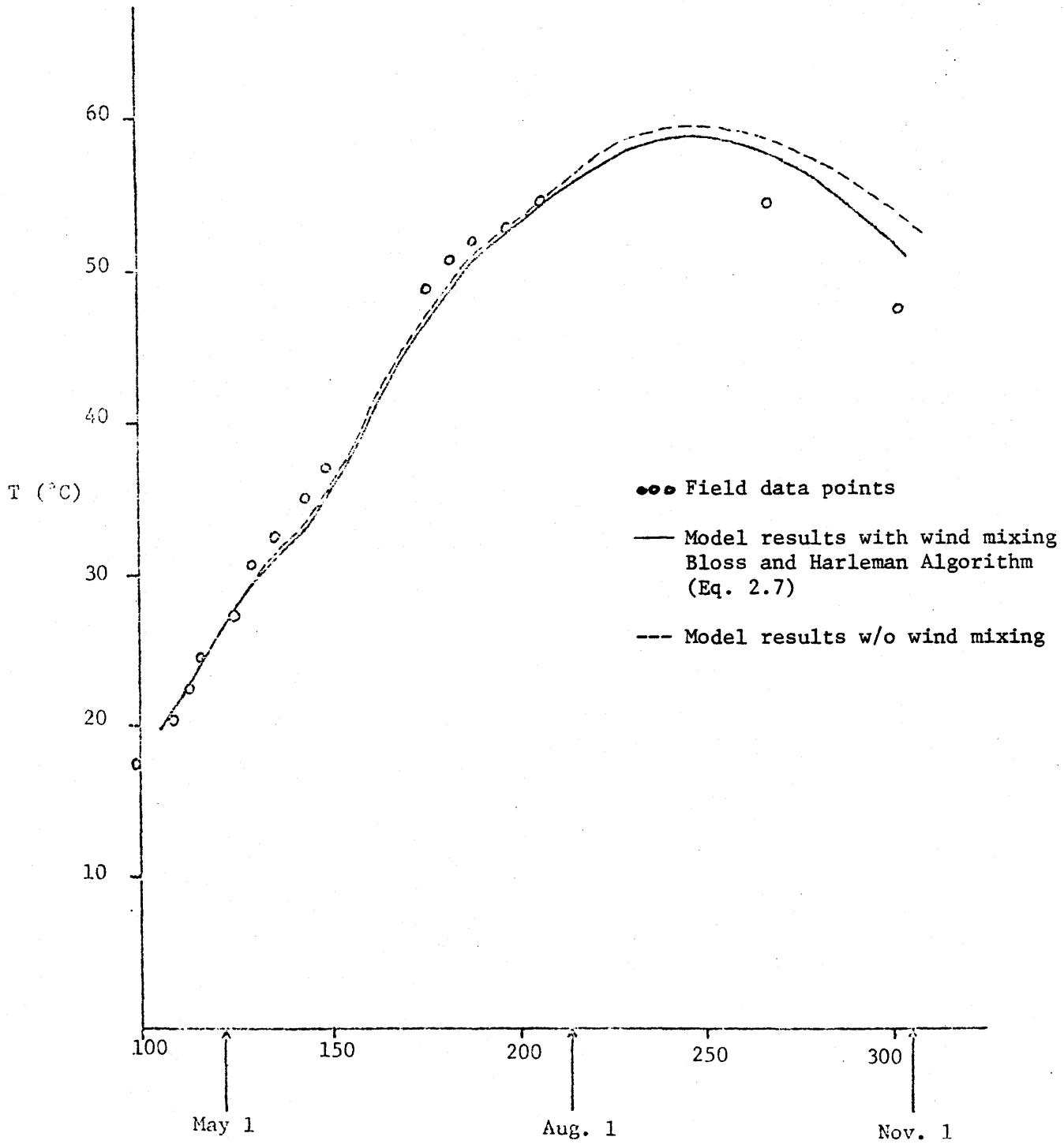

Fig. 2.3 A Comparison between Numerical Model Results and Field Data of the Average Storage Zone Temperature for Wooster, Ohio Solar Pond (155m^2, 3m deep) (19).

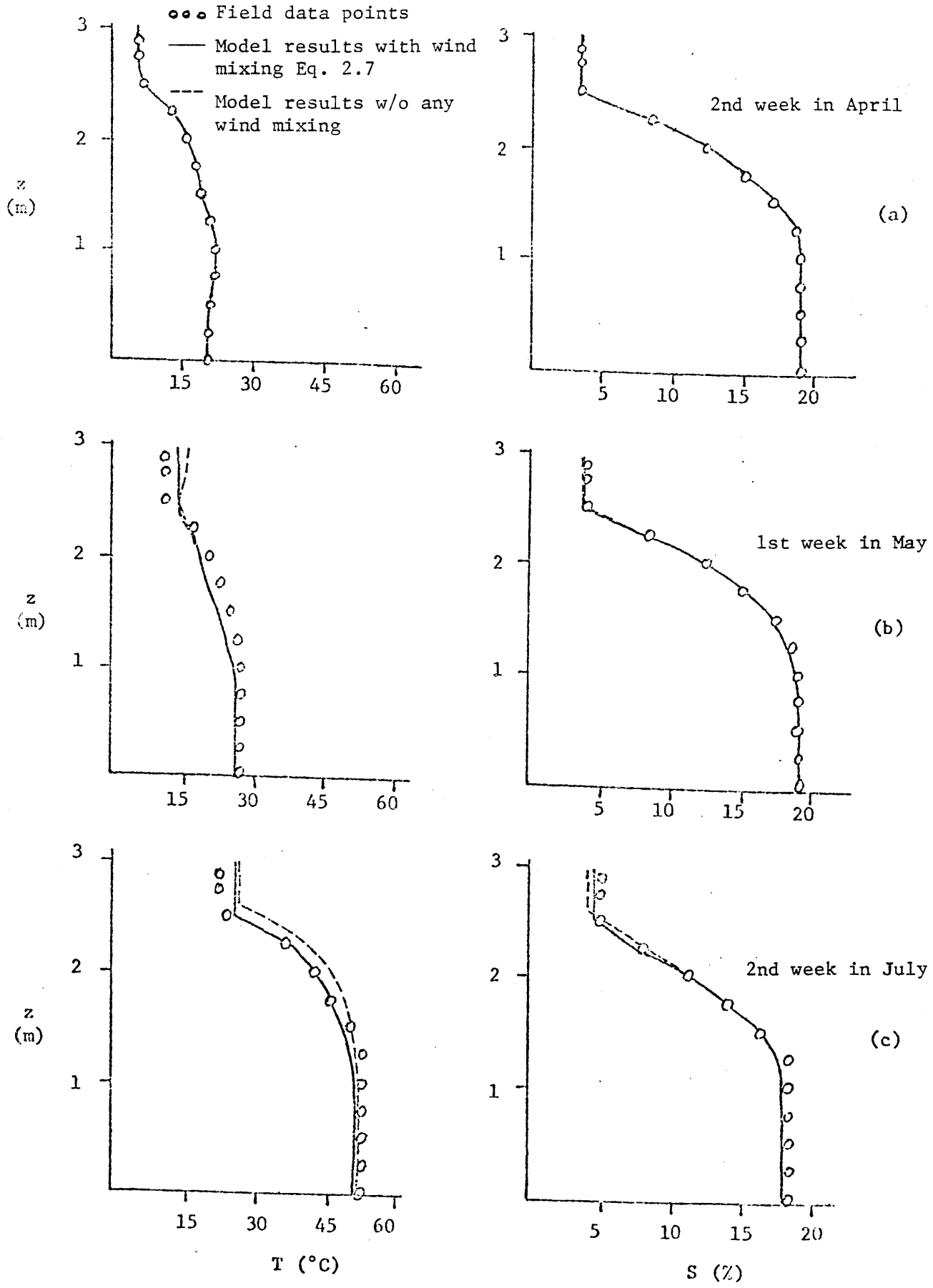

Fig. 2.4 A Comparison between Numerical Model Results and Field Data. for 155m^2 Solar Pond at Wooster, Ohio (19).

In addition, an automatic meteorological station that records air temperature, solar radiation, wind speed and humidity was installed on the roof. Figure 2.5 shows typical temperature and salinity profiles for this pond. Figure 2.6 gives the thermal history of the BCZ and the UCZ. The maximum temperature of 75°C was recorded in the last week of August in the bottom storage zone. Since then the pool has been gradually cooling in response to the onset of autumn and winter seasons. Since the construction of the pond, maintenance measures were taken only once, when 5.8 cm of the surface zone was siphoned off and replaced by 11.8 cm of tap water. The thermal behavior of the pond will be monitored during the winter of 1982-1983.

Mixing in the Dead Sea

An important test of the wind mixing capability of the solar pond model at very large scale is currently underway at MIT. Vertical temperature, salinity and density profiles at monthly intervals have been obtained for the Dead Sea (Israel) from the fall of 1979 through the fall of 1981.

As a result of diversion of fresh water from the Jordan River for irrigation purposes, the Dead Sea became vertically mixed for the first time in the winter of 1979. The winters of 1979-80 and 1980-81 were unusually wet and the temperature and salinity profiles during the periods from December through April show an appreciable amount of vertical mixing of the fresh water that entered during these periods. The Dead Sea has a surface area of approximately 800 km^2 and this data therefore represents an interesting test of the MIT model.

Laboratory Experimental Work

The main thrust of the current laboratory experimental work is to develop a wind mixing model which would be applicable to large solar ponds. The program consists of two basic parts: one, a grid-mixing experiment in a small laboratory tank in which an oscillating grid is used to input energy at the surface; and two, a wind mixing experiment in a 30 m long wind tunnel. The object of the grid experiments is to determine conditions under which double diffusive processes become important relative to turbulence and to parameterize these processes. The wind tunnel experiments will serve as a further check on grid results. Further, the wind tunnel experiments will be used to test different wind mixing suppression systems which will be useful in designing solar ponds.

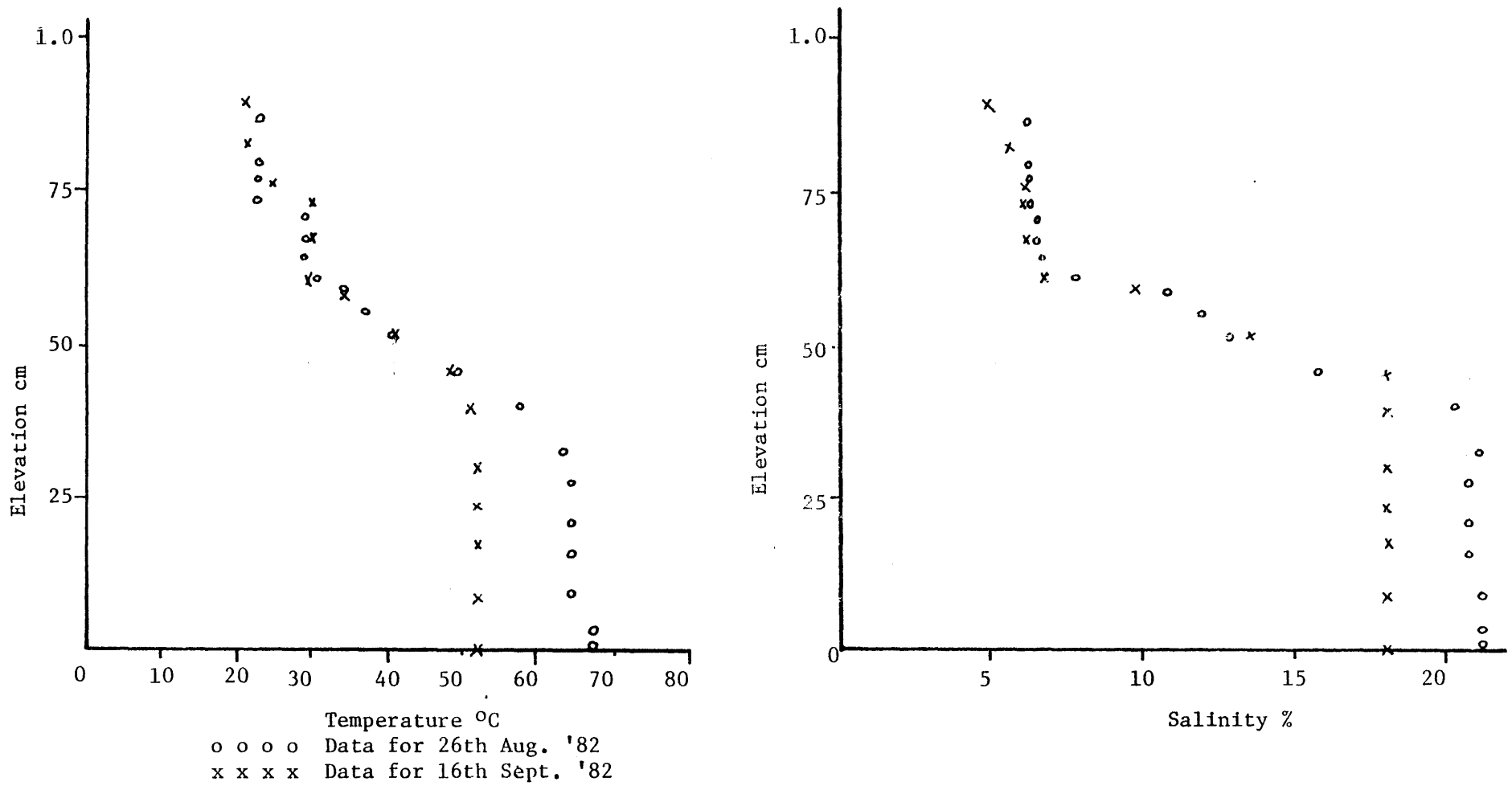

Fig. 2.5 Typical Temperature and Salinity Profiles for the Parsons Laboratory Experimental Solar Pond

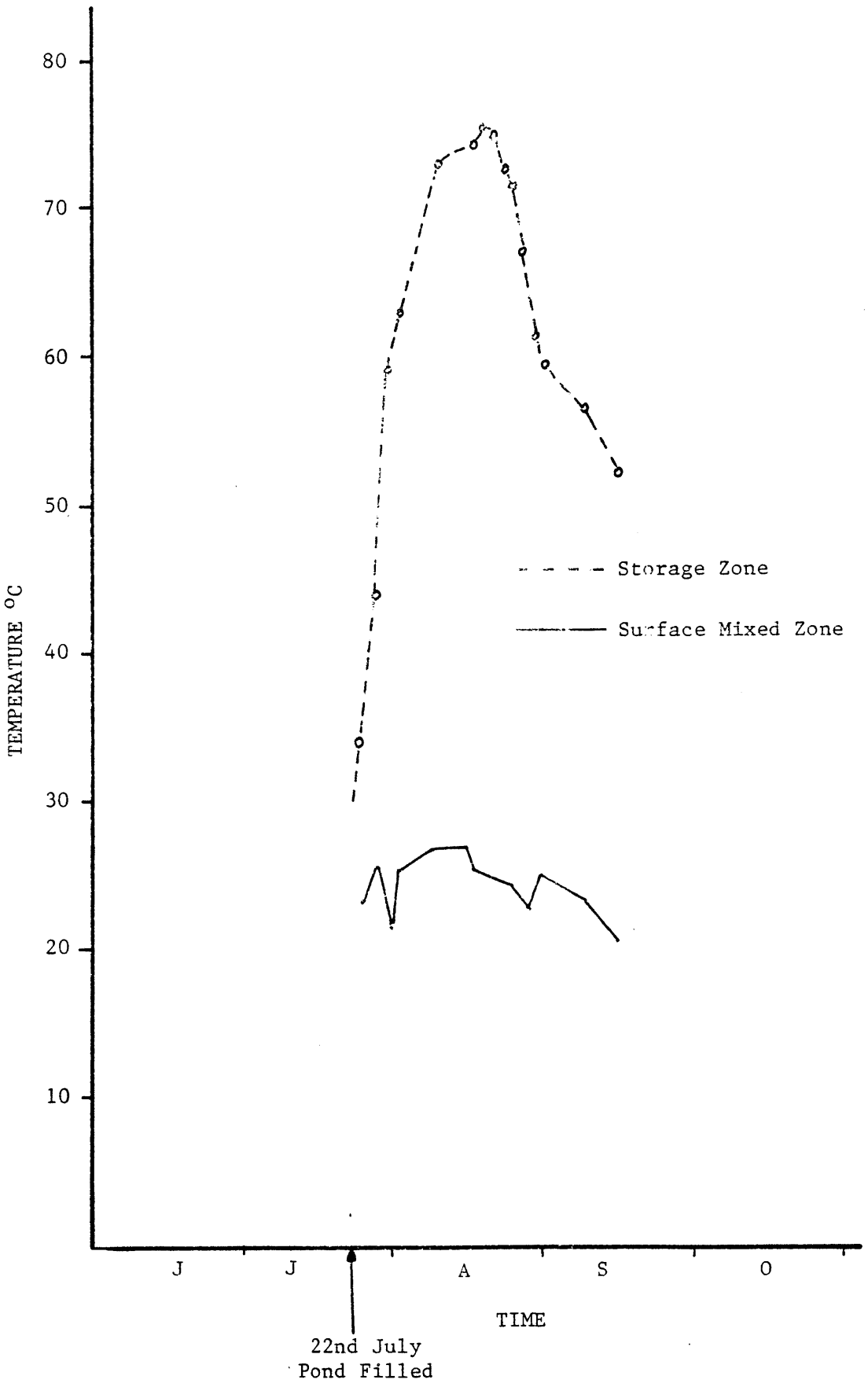

Fig. 2.6 Thermal History of the Bottom Storage Zone and the Surface Mixed Zone for Parsons Laboratory Solar Pond.

Nomenclature

A = area (m^2)

C_p = heat capacity of water at salinity S and temperature T ($W\ s\ kg^{-1}\ {}^oC^{-1}$)

g = gravitational acceleration ($m\ s^{-2}$)

h = mixed layer depth (m)

k_s = molecular salt diffusivity ($m^2\ s^{-1}$)

k_T = molecular thermal diffusivity ($m^2\ s^{-1}$)

L_V = latent heat of evaporation ($Ws\ kg^{-1}$)

q_i = inflow per unit width ($m^2\ s^{-1}$)

q_o = outflow per unit width ($m^2\ s^{-1}$)

S = salinity weight of salt / weight of solution (%)

S_i = salinity of inflow (%)

t = time (t)

T = temperature in the water body (^oC)

T_i = temperature of inflow (^oC)

u_* = friction velocity ($m\ s^{-1}$)

w = vertical velocity ($m\ s^{-1}$)

z = vertical coordinate (m)

ρ = density of water at salinity S and temperature T ($kg\ m^{-3}$)

ρ_o = reference density $kg\ m^{-3}$

ρ_s = density of the water surface hg/n^{-3}

ν = kinematic viscosity ($m^2\ s^{-1}$)

ϕ = solar radiation penetrating the water body ($W\ m^{-2}$)

ϕ_e = evaporative flux from surface ($W\ m^{-2}$)

ψ = precipitation ($m\ s^{-1}$)

3. Large Scale Solar Pond Potential in Egypt

Introduction

This chapter investigates the potential and technical feasibility of constructing and operating large scale solar ponds in Egypt. Potential sites exist in the Qattara Depression, the brine lagoons near Alexandria and Lake Qarun. However, a detailed survey to locate the best site has not been conducted. For the purposes of this study, the Qattara Depression is proposed as the potential large scale development site for two reasons. First, a conventional hydropower generating facility (of the order of 350 MWe base load) has been proposed at Qattara using water diverted from the Mediterranean Sea at a flow rate of 600 m^3/s. It is of interest to compare the electric power potential of large scale solar ponds with a conventional hydropower generating facility. Second, we have had previous experience with the hydrologic and topographic conditions prevailing in the Qattara region (22). Since the factors influencing the performance of solar ponds do not vary significantly with location in lower Egypt, the results should be applicable with slight modifications to the other sites mentioned above.

Calculations and other details are based on a 350 MWe base load power generating facility. However, by installing larger turbogenerators, pumps, etc., it would be possible to generate peaking power two to three times the base load capacity. The proposed scheme consists of five similar solar pond modules. The following section considers the requirements and the availability of resources at this site.

Insolation

Owing to the large thermal inertia of solar ponds, calculations of thermal behavior are usually based on monthly averages of solar radiation incident on the horizontal water surface. Solar radiation measurements for a number of locations in lower Egypt are tabulated in Table 3.1. The best estimates for the Qattara Depression, computed using regression analysis, (23) are plotted in Figure 3.1. The radiation values for Lake Qarun (Shakshuk) and the Qattara Depression are almost identical. Thus very similar thermal behavior is expected of ponds located in the vicinity of these two sites.

Other Meteorological Conditions

Table 3.2 gives the best estimates of other relevant meteorological variables for the Qattara site. The monthly average wind speeds are not excessive; however, transient gusts of wind could cause the deepening of the upper convecting zone. It is expected that this could be controlled by appropriate maintenance measures. The duration of sunshine hours and negligible annual precipitation are indicative of clear sky conditions for the entire year.

Land

Figure 3.2 shows the location of Qattara Depression. The "dotted" position is covered with "sabka" (salt crusts formed by evaporation of brackish water) and is expected to be relatively impermeable. In addition its accessibility and relative proximity to power demand centers makes it a promising site for locating unlined solar ponds. Since the land is barren and uninhabited, it would be available at essentially zero cost. These considerations favorably affect the benefit to cost ratio.

Table 3.1 Average Daily Solar Radiation for Lower Egypt (22)

	Measured Insolation W/m^2			(Computed)
MONTH	SHAKSHUK	ALEXANDRIA	OASIS SIWA	QATTARA
JAN	144	134	149	143
FEB	188	178	193	187
MAR	235	288	234	234
APR	280	278	279	280
MAY	307	309	308	306
JUN	323	324	323	325
JLY	316	317	318	316
AUG	295	297	299	297
SEPT	257	253	259	257
OCT	208	202	210	207
NOV	159	151	162	158
DEC	133	121	135	131
MEAN	237	233	239	237

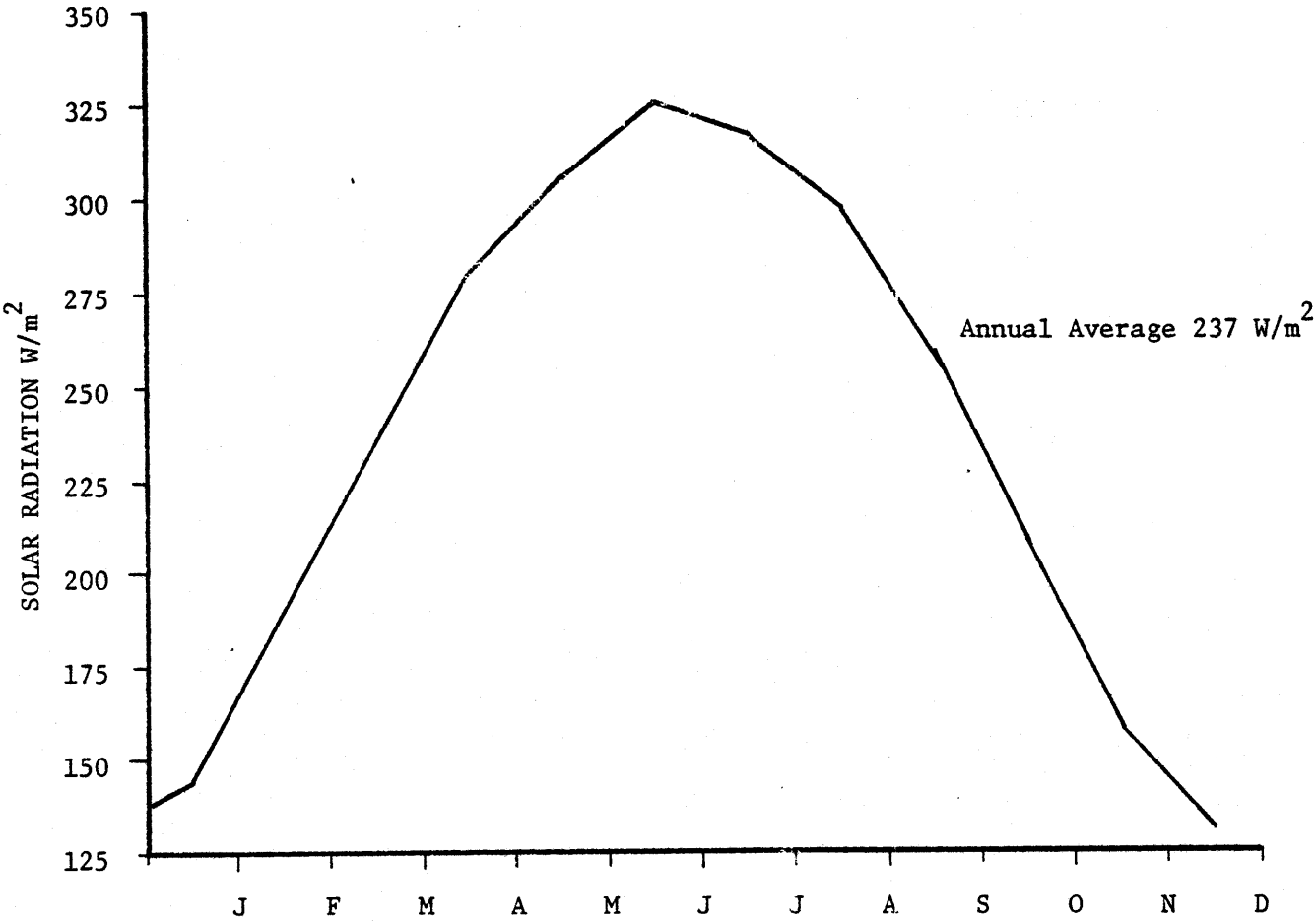

Figure 3.1 Best Estimate of Incoming Solar Radiation for the Qattara Site

Table 3.2 Best Available Estimates of Meteorological Data for the Qattara Site (23)

MONTH	RAIN	AIR TEMP.	RELATIVE HUMIDITY	WIND SPEED	SUNSHINE DURATION
	mm/mo.	^{o}C	%	m/s	hr/day
1	3.3	13.3	68.0	2.3	7.2
2	3.7	15.0	68.0	2.8	8.0
3	2.2	17.2	64.0	3.5	8.8
4	0.7	20.6	61.0	3.8	9.7
5	1.5	24.1	58.0	3.9	10.6
6	0.0	26.4	55.0	4.1	12.1
7	0.0	28.2	58.0	3.3	12.0
8	0.0	28.5	59.0	3.2	11.4
9	0.0	26.8	62.0	3.6	10.4
10	2.8	23.4	60.0	3.2	9.1
11	2.4	19.5	64.0	2.5	7.2
12	5.1	14.8	67.0	2.5	7.2
MEAN	1.8	21.5	62.0	3.3	9.5

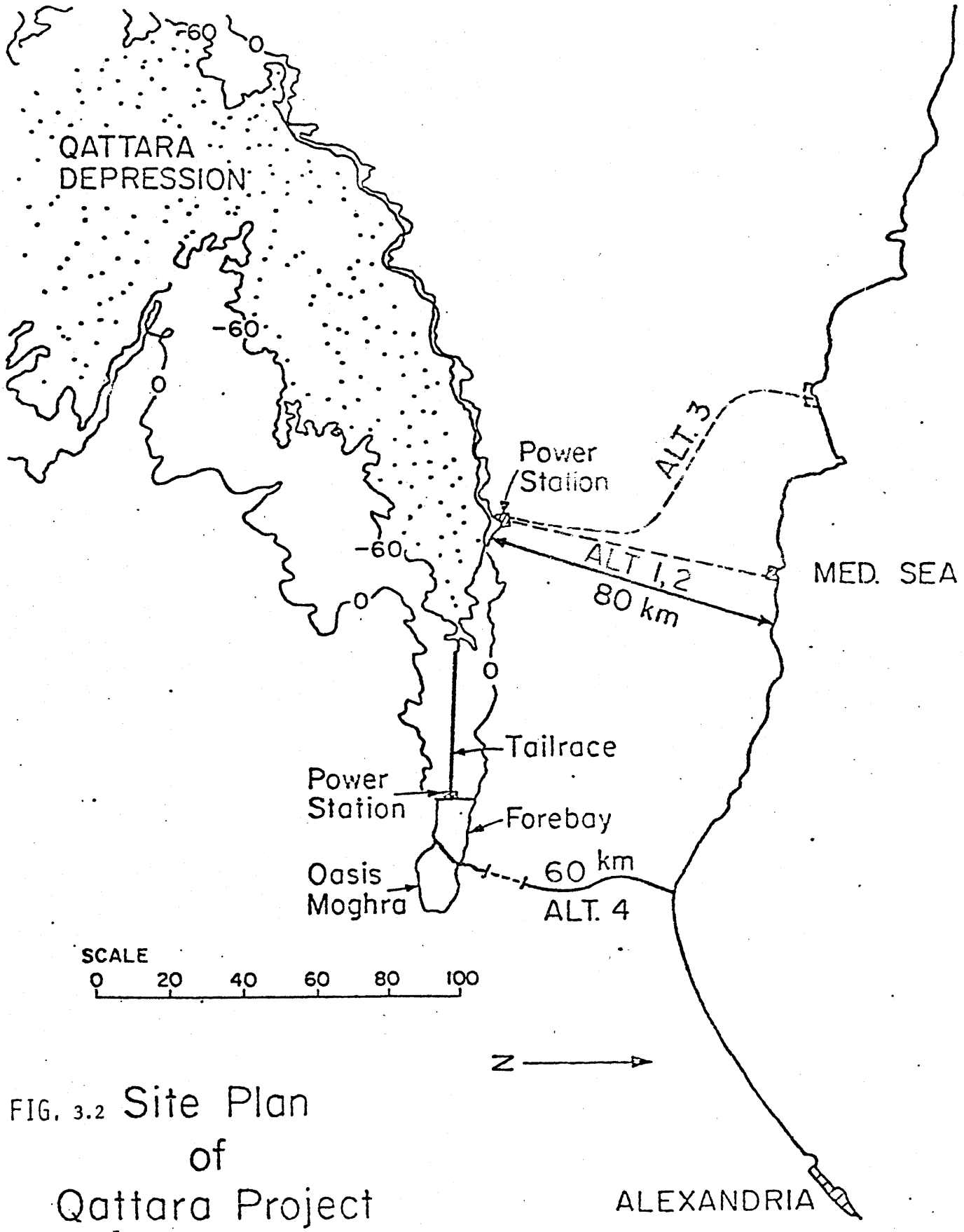

FIG. 3.2 Site Plan of Qattara Project

The total area required for a 350 MWe solar pond electric generating plant is of the order of 350 km^2 including 250 km^2 of evaporation ponds and 100 km^2 of solar ponds. This is approximately 3% of the 12,000 km^2 area of the depression at 60 mbsl (the approximate equilibrium level of the lake which would be formed if the proposed Qattara hydroelectric project is enacted). Each of the five solar pond modules consists of a 20 km^2 solar pond and a 50 km^2 evaporation pond. The exact layout and the location of the system would require a detailed topographic and geotechnical survey. Figure 3.3 gives a conceptual layout for the solar pond system. The area with minimum seepage and earthwork would be the most cost effective.

Salt

Figure 3.4 illustrates the proposed salinity profile for the solar pond. Table 3.3 presents the salt and brine requirements for the initial filling of a 20 km^2 pond. These large quantities of salt may be obtained by diverting water from the Mediterranean Sea at a rate of 14 m^3/s and subsequently evaporating it within the Depression.

Table 3.3 Salt and Water Requirements for a 20 km^2 Solar Pond Module (70 MWe)

Layer	Depth m	Salinity* %	Volume m^3	Weight of Salt kg
UCZ	0.5	6%	1.0×10^7	6.3×10^8
CZ	1.0	6%-20% (Linear Gradient)	2.0×10^7	2.8×10^9
BCZ	1.5	20%	3.0×10^7	6.8×10^9

*Expressed as weight of salt/weight of solution.

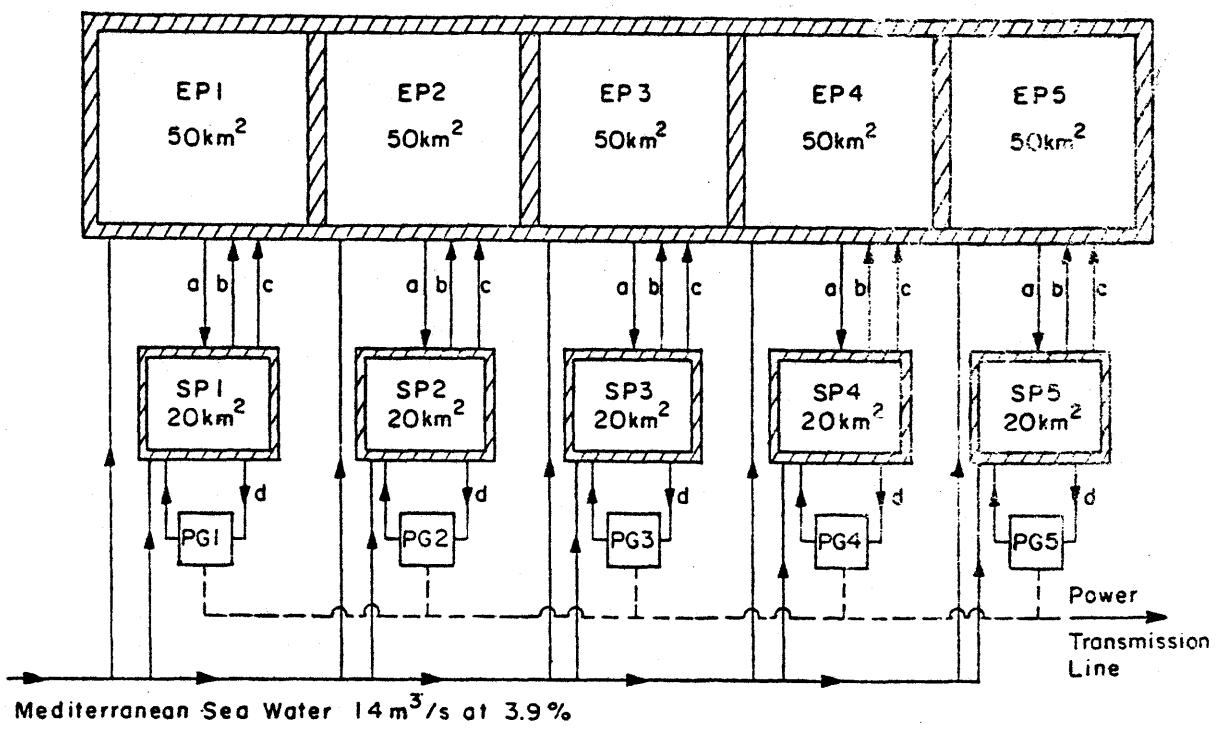

LEGEND

SP	Solar Pond	
EP	Evaporation Pond	
PG	Power Generating Facility	
→	Flow of Brine / seawater	
a →	Saturated Brine from EP to BCZ	0.1 m³/s @ 23%
b →	Salt Water flushed from UCZ to EP	1.8 m³/s @ 6%
c →	Brine from BCZ to EP	0.1 m³/s @ 20%
d →	Hot Brine for Heat Extraction	39.5 m³/s

Figure 3.3 Conceptual Layout of 370 MWe Solar Pond Facility at Qattara

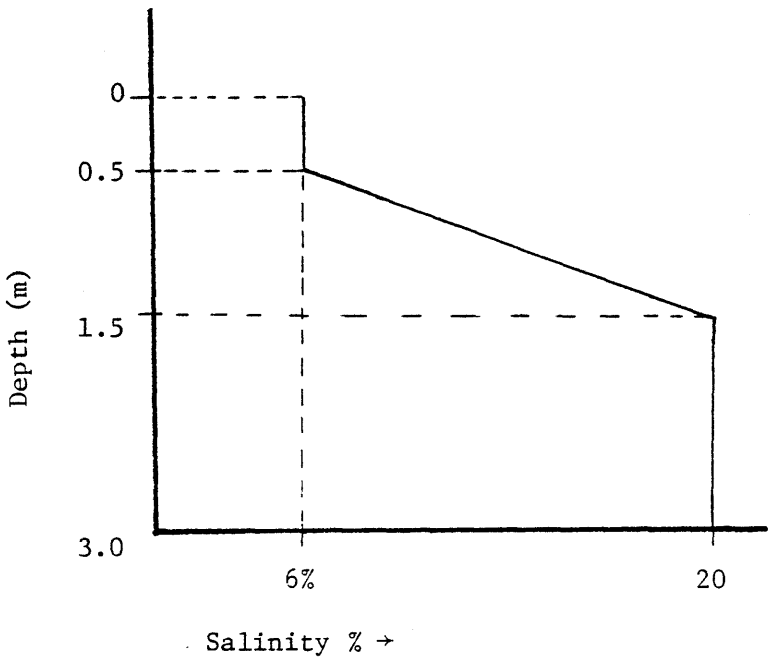

Figure 3.4 Proposed Salinity Profile for the Solar Pond at Qattara

Three factors govern the time required to produce enough brine to start the solar ponds. These are the total area available for concentrating the sea water (including both evaporation ponds and unused solar ponds), the rate of inflow of sea water and the rate of evaporation which is dynamic in nature owing to its dependence on the salinity of water and the local meteorology. Therefore, the minimum time required to produce enough brine using the available resources is an interesting and important dynamic programming problem. Preliminary calculations indicate that enough brine would be available to start the first pond in about a year and eight months. These calculations are based on the availability of an area of 350 km^2 (five solar ponds, each 20 km^2; and five evaporation ponds, each 50 km^2), continuous inflow of sea water at 14 m^3/s and 3.9% salinity, an annual average evaporation rate of 1.4 m (over a salinity range of 3.9% to 23%) absence of seepage and the availability of facilities to pump saturated brine from pond to pond.

On an average, one additional pond could be added every year so that at the end of five years all ponds would be operational. After this period the diverted water would be used for surface flushing.

The diversion of 14 m^3/s of water from the Mediterranean Sea is less than 3% of the discharge envisioned for hydroelectric generation of an equivalent amount of base load power, by the proposed Qattara Hydroelectric Project (22). If the hydroproject is enacted, the small amount of additional sea water flow required for the solar ponds could easily be diverted at the tailrace. If not, the solar pond flow could be conveyed by a relatively small concrete or plastic pipe following the route of Alternative 1 or 2 (Figure 3.2). In this case, additional power of the

order of 7 MWe could be generated by installing a hydropower plant to utilize the 60 m drop between the Meditteranean Sea and the solar ponds.

Water

After the initial filling of the ponds a continuous supply of sea water at the rate of 2.8 m^3/s per pond (14 m^3/s for five ponds) is necessary to maintain the thickness and salinity of the UCZ. Of this, approxiatemly 1.0 m^3/s/pond, evaporates. The remaining 1.8 m^3/s is flushed out into evaporation ponds and concentrated to produce brine for maintaining the salinity of the BCZ. The size of the evaporation ponds (50 km^2) is such as to evaporate the entire volume of water flushed out of the solar ponds.

Pond Performance

The performance of the solar ponds was simulated for an initial period of 2 years using the solar pond model developed at MIT (19). A time step of one day and a grid size of 0.25 m was used. The initial salinity profile was assumed as in Figure 3.4 and temperature was assumed homogeneous throughout. Figure 3.5 shows the predicted temperature variation for a period of two years with heat extraction from the BCZ at a uniform rate of 812 MW(th). A maximum bottom layer temperature of about 80°C is predicted at the end of summer and a minimum of 45°C is predicted at the beginning of spring. Since the pond does not reach a steady state after the first year, the predicted temperatures for the second year are different from those of the first. The model does not account for heat loss to the ground and to that extent overpredicts the temperature slightly. Figure 3.6 shows a series of temperature profiles obtained from the model.

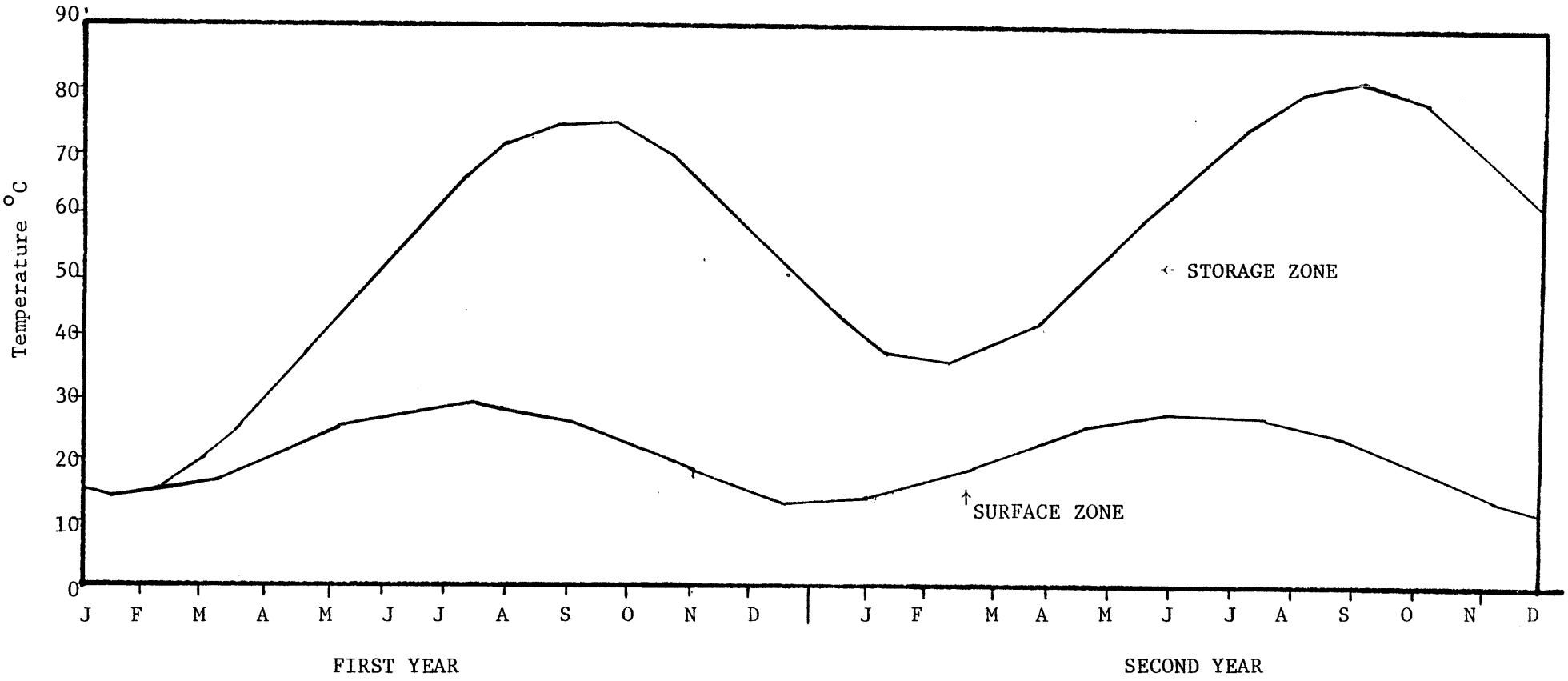

Figure 3.5 Predicted Temperatures for a 20 km^2 Solar Pond at Qattara with Heat Extraction @ 812 MW(th)

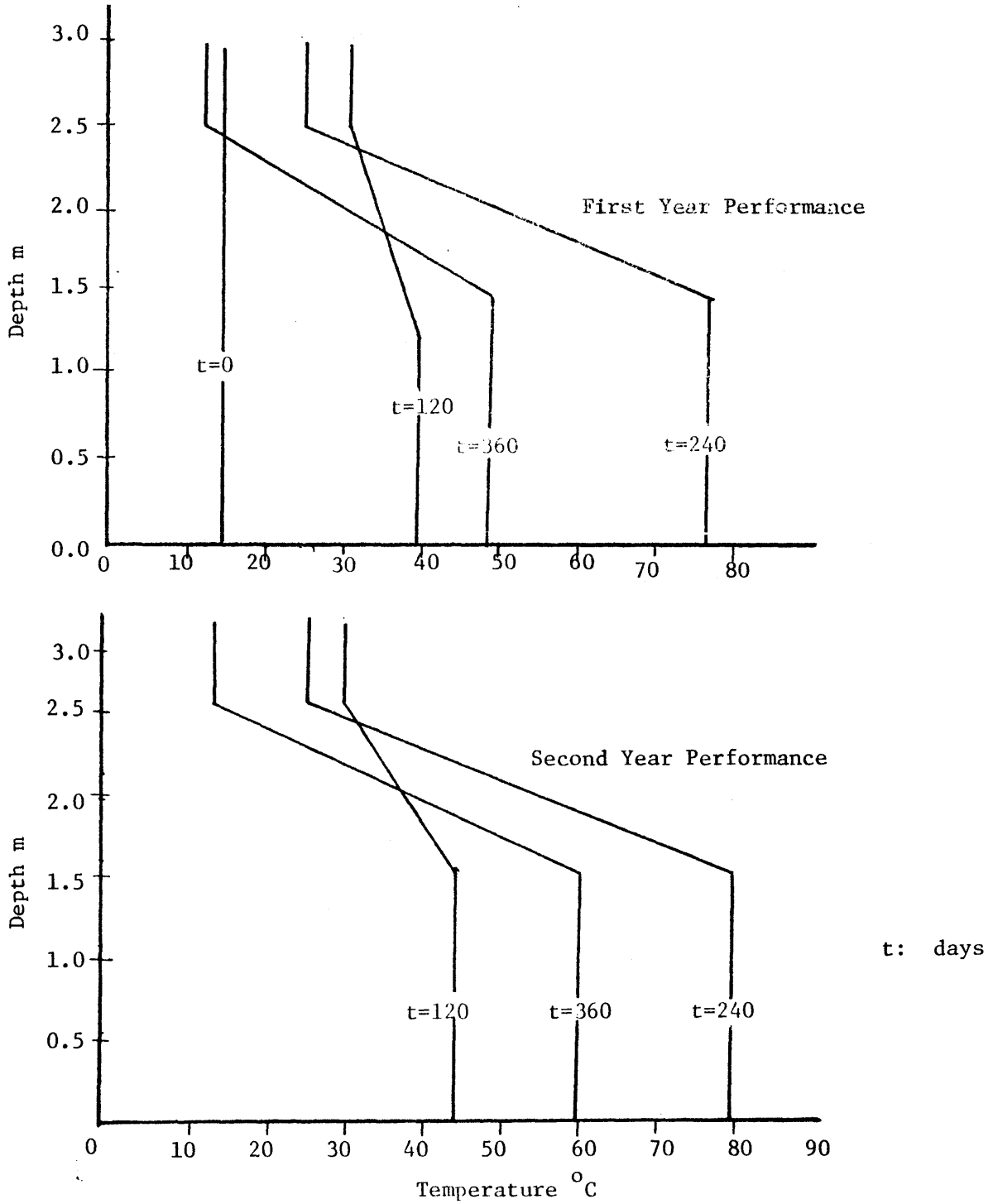

Figure 3.6 Predicted Temperature Profiles for a 20 km^2 Solar Pond at Qattara with Heat Extraction at 812 MWth

Energy Budget

A detailed energy budget for a 20 km^2 pond is given in Table 3.4. Incident solar energy is assumed to penetrate the pond as per Eq. 1.1 with $\eta = 0.5\ m^{-1}$ and $\beta = 0.5$. About 22% of the insolation reaches the BCZ. A portion of this is lost to the gradient zone (GZ) and the ground by conduction. After a steady state has been reached, heat loss to the ground would be negligible. Losses through the GZ account for 5% of the incoming radiation or 22% of the energy penetrating the BCZ. The remaining 17% of incoming radiation is available for extraction.

As per the model prediction, brine is extracted at an annual average temperature of 65°C. With the annual average temperature of the evaporation ponds (also used as the condenser water heat sink) of 22°C, the ideal annual average Carnot cycle efficiency is calculated as

$$C_c = (1 - \frac{273+22}{273+65}) = 12.7\% \qquad (3.1)$$

However, practically realisable efficiency is only about two-thirds of C_c. Thus the thermal to electrical conversion efficiency is about 8.5%. With the above assumptions pond output is calculated in Table 3.4 to be 70 MWe.

Water and Salt Balances

Figure 3.7 illustrates the overall water balance for the solar pond. Water balance for the UCZ has been discussed earlier. Hot brine from the BCZ is passed through a heat exchanger to vaporize the working fluid (freon or ammonia) that drives the turbine. Assuming a 5°C drop across the heat exchanger, a flow rate of 39.5 m^3/s is sufficient to transfer 812 MWth to the working fluid. In addition, 0.1 m^3/s of brine is extracted from the

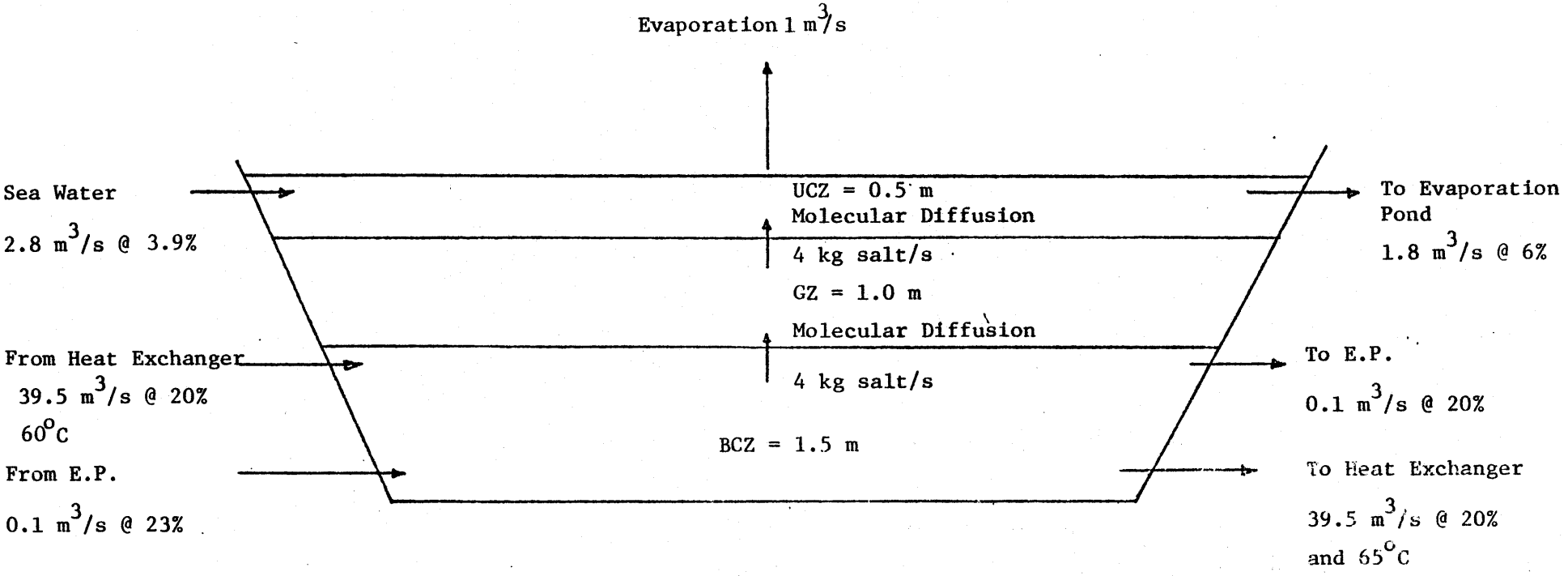

Figure 3.7 Water Balance for a 20 km^2 Solar Pond

Table 3.4 Energy Budget for a 20 km^2 Solar Pond at Qattara (70 MWe)

Incoming Solar Energy (Figure 3.2)	4740 MW	(237 W/m^2)
Energy penetrating to the BCZ (Eq. 1.1) ($z = 1.5$ m, $\beta = 0.5$, $\eta = 0.5\ m^{-1}$)	1052 MW(th)	
Energy loss due to conduction	240 MW	
Thermal to Electric Conversion Efficiency		
67% of ideal Carnot cycle efficiency with ($T_{SOURCE} = 65^oC$ and $T_{SINK} = 22^oC$)	8.5%	
Electric Power Output (base load)	70 MWe	
Net Power Density	3.5 MWe/km^2	
Overall Efficiency		
$\frac{\text{Net electric power}}{\text{Incident Power}} * 100$	1.5%	

BCZ and concentrated to a salinity of 23% in the evaporation pond before returning to the BCZ. This assumes that the BCZ is concentrated continuously, though periodic concentration of the BCZ is also possible. In all cases, the diffusion at the inlets and outlets should be designed to prevent mixing of the three zones.

Evaporation Pond

The evaporation pond was sized to evaporate the entire water flushed out of the UCZ. For the purpose of maintaining the BCZ salinity only, it is possible to have a smaller evaporation pond. However, this would increase

the start-up time for the solar pond and would require an additional water body, for example an existing lake, to dispose of part of the water flushed out of the UCZ. In this case, the reduced cost of pond construction has to be weighed against the longer gestation period for the project. Figure 3.8 illustrates the water and salt balances for the evaporation pond. The precipitated salt may be allowed to accumulate in the evaporation pond or could be periodically harvested and put to some use.

Cost of Solar Pond Facility

The costs involved in the construction of solar ponds include earthwork for building the pond, cost of the pipeline to transport water from the Mediterranean Sea (in the absence of the conventional hydro project), the cost of turbogenerator, pumps, heat exchanger, etc. A detailed site-specific economic survey is essential to arrive at an estimate of the costs involved. Such a large scale solar pond system has not been constructed to date and, therefore, it is not possible to quote figures from past experience. However, ballpark estimates may be obtained from past studies. Using estimates from Tables 1.1, 1.2 and 1.3 and considering the favorable Egyptian conditions, the 100 km^2 350 MWe solar pond plant might cost in the vicinity of $1 billion.

One of the most important parameters in the construction, maintenance and operation of a solar pond facility is the rate of evaporation. This affects the start-up time, the flushing water requirements and the sizing of the evaporation ponds. In order to accurately estimate evaporation at the Qattara Depression it is necessary to collect site specific meteorological data. We belive that the installation of an automatic or manned meteorological station in the Qattara depression is of prime im-

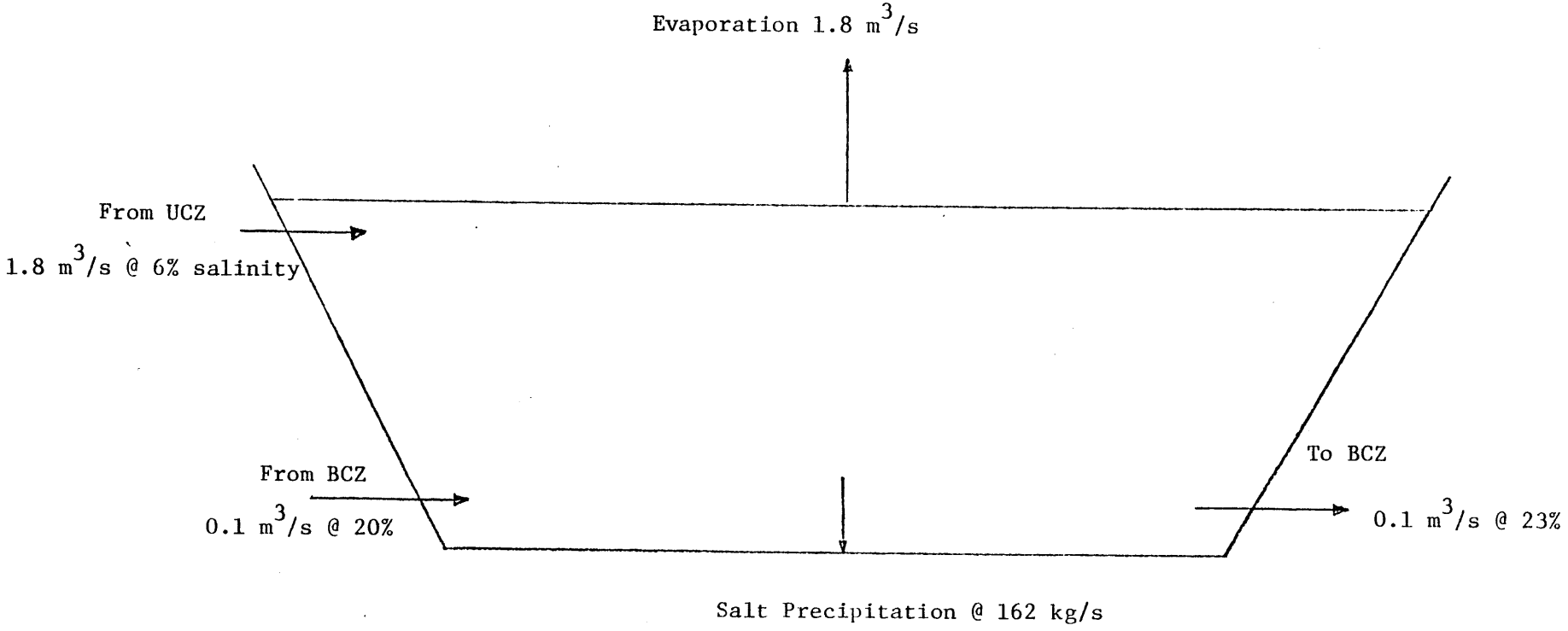

Figure 3.8 Water Balance for 50 km^2 Evaporation Pond

portance for the efficient sizing of the solar pond facility. The data collection system should preferably start a few years ahead of the construction of the solar ponds. Relevant here is the fact that the data collected would also be very useful for the proposed conventional hydropower project.

Before embarking on a large scale solar pond system, it would be advisable to build a small demonstration pond to acquire first hand local experience with solar ponds. The setting up of such a facility is described in the next chapter.

4. Demonstration Pond

Introduction

This chapter considers two possible sites for setting up demonstration ponds in Lower Egypt: Lake Qarun and Lake Maruit. Both these sites have all the necessary resources for the construction and operation of a solar pond. Lake Maruit has the added advantage of not requiring the construction of large evaporation ponds, which are already in existence.

Lake Qarun (Fig. 4.1) has an area of 248 km^2 with an average depth of 4.2 m. The salinity of the lake (about 4%) is approximately the same as that of the Mediterranean water, so that the procedures for concentrating the brine would be similar to those required at the Qattara Depression or any other site using sea water as a brine source. Inflow to the lake is primarily return flow from irrigation with a salinity of 0.1%.

Lake Maruit is located to the south and west of Alexandria. Presently the El-Nasr Saline Company has evaporation ponds covering an area of 25 km^2 of the lake. These ponds contain concentrated brines (salinity about 20%) and are situated several meters below sea level. Their average depth is about 1 m. The available brine can be used for the initial filling of the pond as well as for the subsequent maintenance of the BCZ, thus eliminating the necessity to build evaporation ponds. In addition, the proximity of the ponds to the Mediterranean is an added advantage for it provides a convenient source of "fresh" water for the UCZ, and for subsequent surface flushing. In preliminary discussions, the El-Nasr Saline Company have expressed their willingness to cooperate in the construction and operation of a solar pond adjacent to one of their large evaporation ponds. (It should also be mentioned that they have plans to develop an evaporation pond at Abuksa

baylakes on the southern shore of Lake Qarun.)

Pond Size

As an example, a pond 75 m x 75 m with an area of 5625 m^2 and an average total depth of 3.0 m is considered. The pond consists of an UCZ of 0.5 m; a GZ of 1.0 m and a BCZ of 1.5 m. The salinity profile is the same as for the large ponds proposed at Qattara, Figure 3.4. Table 4.1 gives some additional details of the pond. The depth and the salinities of UCZ and BCZ are maintained by surface flushing and periodic or continuous addition of saturated brine (salinity 25%) to the BCZ.

The remaining discussion focuses on a pond at Lake Qarun. However, similar considerations apply for a pond in Lake Maruit except that the flushing flow would come from the Mediterranean Sea and the brine flow from adjacent evaporation ponds.

Figure 4.2 gives an overall water balance for a solar pond on Lake Qarun. Once the pond is in operation, a continuous discharge 82 m^3/day from the lake would be required to flush the UCZ. Of this 28 m^3/day is lost by evaporation and the remaining 54 m^3/day flows to the evaporation pond. The salinity of the BCZ is maintained by extracting 2.3 m^3/day of brine at 20% salinity and replacing it with an equivalent volume of saturated brine at 23% salinity. The saturated brine is obtained from the evaporation pond as discussed subsequently.

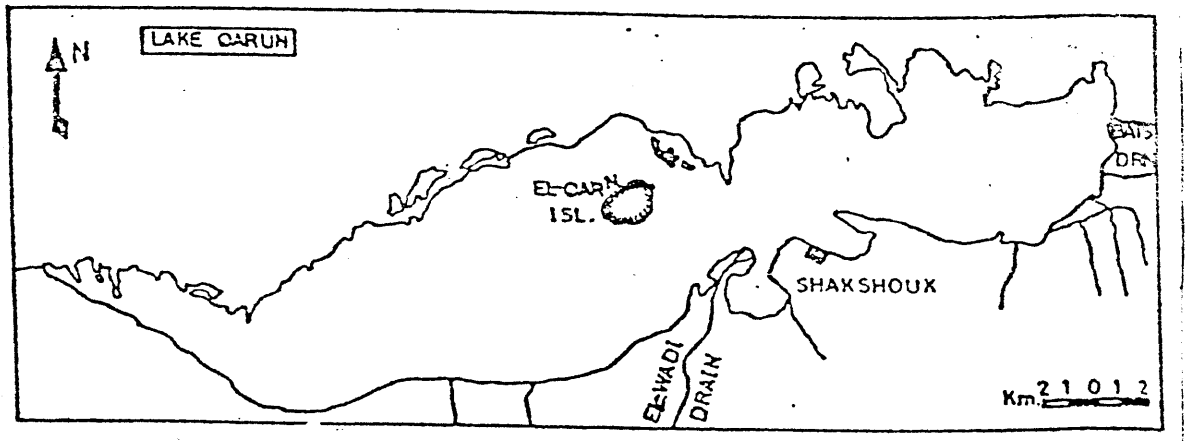

Area	248 km^2
Mean Depth	4.2 m
Surface Elevation (1980)	-44.3 m
Salinity (1980)	3.9%
Annual Evaporation	1.9 m

Figure 4.1 Map Showing Lake Qarun and Shakshuk Meteorological Station

Table 4.1 Details of a Demonstration Pond

Layer	Depth	Salinity	Volume	Salt Content
	m	%	m^3	kg
UCZ	0.5	6.0	2813	$1.8*10^5$
GZ	1.0	6.0-20.0 (Linear variation)	5625	$7.9*10^5$
BCZ	1.5	20.0	8438	$1.9*10^6$
TOTAL	3.0		16,876	$2.9*10^6$

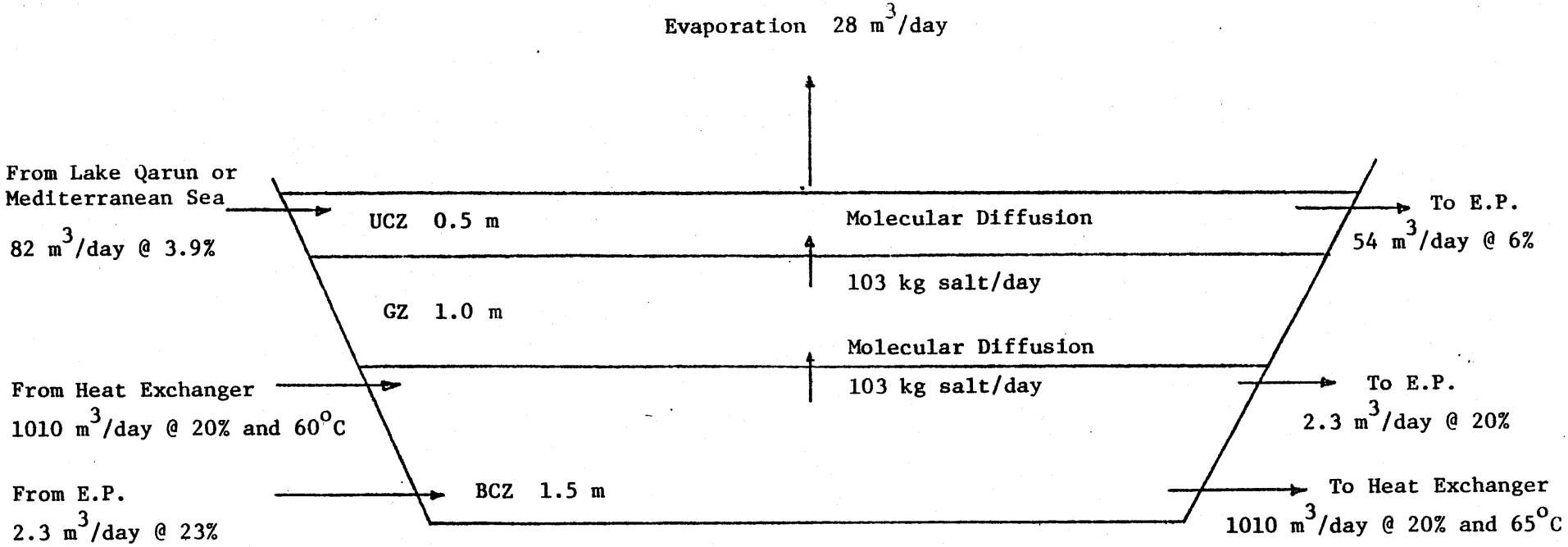

Figure 4.2 Daily Water Balance for the Demonstration Pond

75 m x 75 m (5625 m^2)

Construction of the Facility

The first step in the construction of the pond is the selection of the site. The ponds should be located at a place where seepage into and out of them will be negligible. Further the site should be easily accessible. One possible location is near Shakshuk where a meteorological station is in operation. At such a site, heat extracted from the solar pond could be used to meet the hot water requirements of nearby hotels.

Civil work for the facility includes building of dikes, inlet and outlet diffusers for flushing and extraction of hot brine, piping system and pumping stations, installation of heat exchangers, and turbogenerator and electrical transmission system if electricity is to be produced. An efficient design of this system would require a detailed land and bathymetric survey of the site. A preliminary conceptual layout, considering a pond on Lake Qarun, is illustrated in Figure 4.3.

Evaporation Pond

For a pond on Lake Qarun, an evaporation pond is necessary to produce enough brine to start the solar pond and, once the pond is in operation, to produce saturated brine for concentrating the BCZ. The size of the evaporation pond is an important design parameter. For the sole purpose of maintaining the concentration of the BCZ at 20% salinity, a small evaporation pond 430 m^2 in area is sufficient. However, with an evaporation pond of this size, the start up time is of the order of eight years which is clearly very undesirable for a demonstration pond. A larger evaporation pond with an area of 14400 m^2 is proposed.

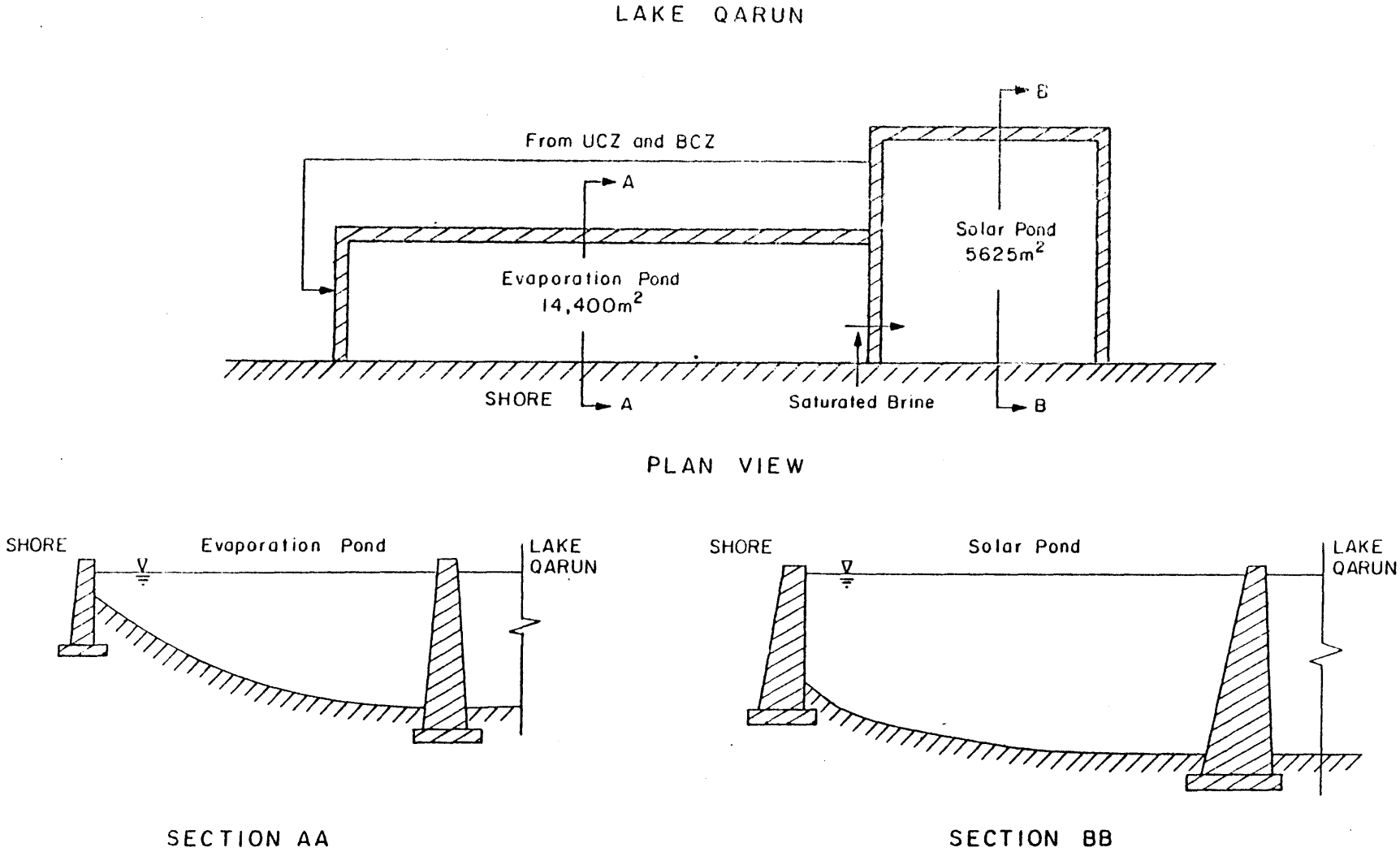

Fig. 4.3 Conceptual Layout of Solar Pond Demonstration Facility at Lake Qarun

Figure 4.4 illustrates water and salt balance for the evaporation pond. Inflows to this pond consist of 2.3 m^3/d from the BCZ and 54 m^3/d flushed from the UCZ of the solar pond. The salt balance indicates a daily precipitation of 3,280 kg of salt which is a useful byproduct. For a pond in Lake Qarun, this would also help in reducing the rate of increase of lake salinity. The start-up time with an evaporation pond of this size is of the order of two years. It is noted that there exists a tradeoff between the start-up time and the size and hence cost of construction of the evaporation pond. With more specific data it would be possible to find an optimum size of the evaporation pond. Note that for a pond near Lake Maruit, brine is readily available for the initial filling of the pond. The start up time merely consists of the time required to construct the dikes and other civil works.

Pond Performance and Energy Extraction

Important meteorological factors affecting the pond performance at either site are tabulated in Table 4.2. A comparison with the mean meteorological conditions prevailing in the Qattara Depression, Table 3.2, indicates that the three sites are similar. Thus the performance of a demonstration pond at Lake Qarun or Lake Maruit is expected to be very similar to that of large ponds at the Qattara.

Table 4.3 illustrates the energy balance for this pond. Thermal energy of the order of 230 Kw can be extracted on an average annual basis. Assuming a drop of $5^{o}C$ across the heat exchanger, 1010 m^3/day of hot brine has to be pumped from the BCZ through the heat exchanger. The energy extracted can be used to generate electricity using a low temperature Rankine cycle turbine. With 8.5% energy conversion efficiency, from thermal to electrical, a base load of 20 KWe can be generated. Depending on the engineering design, either the evaporation pond or the lake could be used as a sink for waste heat.

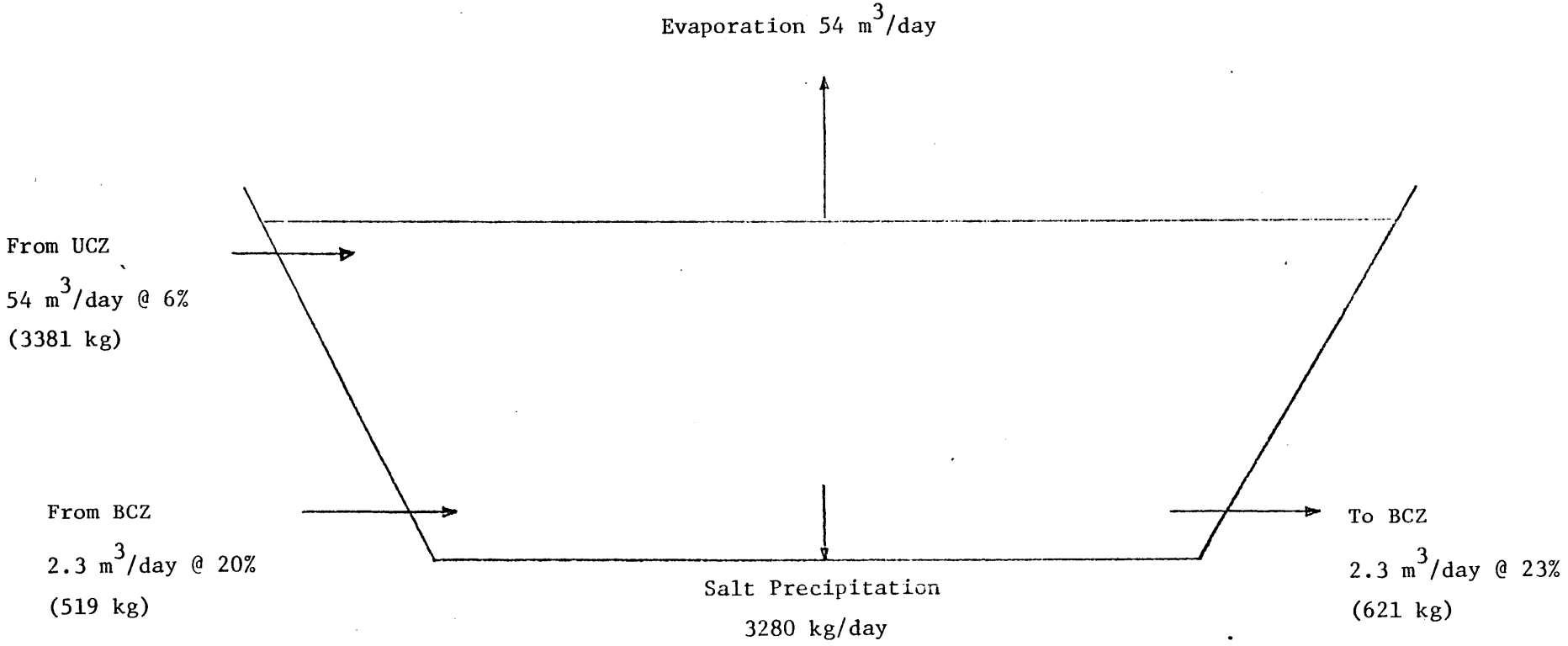

Figure 4.4 Water Balance for Evaporation Pond 14400 m^2 area

Table 4.2a Meteorology of Lake Qarun*

MONTH	AIR TEMP °C	Relative Humidity %	Wind Speed m/s	Sunshine hours hr/day	Rain mm/month
1	13.1	68	2.3	7.2	0.9
2	15.4	68	2.8	8.0	1.4
3	17.8	64	3.5	8.8	1.4
4	21.7	61	3.8	9.7	0.6
5	25.4	58	3.9	10.6	1.1
6	27.4	55	4.1	12.1	0.0
7	29.3	58	3.3	12.0	0.0
8	29.4	59	3.2	11.4	0.0
9	27.4	62	3.6	10.4	0.0
10	23.8	60	3.2	9.1	0.8
11	19.6	64	3.2	8.1	0.5
12	14.6	67	2.5	7.2	4.0
Mean	22.1	62	3.3	9.5	0.9

*Average Daily Solar Radiation tabulated in Table 3.1

Table 4.2b Meteorology of Lake Maruit*

MONTH	AIR TEMP	Relative Humidity	Wind Speed	Sunshine hours	Rain
	°C	%	m/s	hr/day	mm/month
1	13.6	67	4.5	7.0	59.2
2	14.3	65	4.6	7.7	23.2
3	16.1	62	4.9	8.6	11.8
4	18.3	64	4.8	9.8	3.0
5	20.9	68	4.3	11.1	1.1
6	24.0	70	4.5	12.0	tr
7	25.6	71	4.6	12.2	0.0
8	26.4	69	4.5	11.8	0.0
9	25.3	66	4.2	10.5	1.4
10	22.7	66	3.7	9.4	11.8
11	19.4	67	3.8	8.2	24.7
12	15.4	66	4.1	6.7	48.7
Mean	20.2	66	4.4	9.6	15.4

*Average Daily Solar Radiation tabulated in Table 3.1

Table 4.3 Energy Balance for the Demonstration Pond

Incoming Solar Energy (Table 3.2)	1.33×10^3 KW(th) (237 W/m^2)
Energy penetrating to the BCZ, (Eq. 1.1)	
(z = 1.5 m, β = 0.5, η = 0.5/m)	3.0×10^2 KW(th)
Energy loss due to conduction	65 KW(th)
Thermal to Electric Conversion Efficiency	
(67% of ideal Carnot cycle with $T_{source} = 60^oC$, $T_{sink} = 22^oC$)	8.5%
Electric power base load	20.0 KW(e)
Power Density	3.5 KWe/1000 m^2

Cost

At present sufficient site specific data are not available to estimate the construction and the maintenance cost of the facilty. A market survey to collect material and labor costs would be required. However, for comparitive purposes it is noted that some economic data is available for similar sized ponds built in the U.S. For example, the Tennessee Valley Authority Pond in Chattanooga (Table 4.4) cost about $1.6 million. Approximately 50% of the total cost was for liner and salt which would not be required for the Lake Qarun Pond.

Brine requirements for the initial filling of the pond are summarized in Table 4.1. Sufficient brine is obtained by evaporating Lake Qarun water in the evaporation and solar ponds. For this start-up time is of the order of 2 years.

Data Required for a Detailed Analysis

Considerable data will have to be collected before a detailed economic feasibility report and engineering designs can be prepared. This would include:

1) Surveys to estimate the permeability of the soils at the location of evaporation and solar ponds.
2) Experiments to study the effect of hot concentrated brine on the bottom sediments. Chemical reactions causing coloration of the pond or causing effervescence can be harmful to the pond.
3. Detailed analysis of the chemistry of lake water will be required. An accurate relationship between salinity, temperature and density will have to be established.
4. Accurate estimates of evaporation and the effect of salinity on evaporation will be necessary.

Table 4.4 Capital Costs for 4000 m^2 Solar Pond at Chattanooga, U.S. (Ref. 23)

Capital costs for a ten-acre NCSP were broken down as follows:

Land Cost	$ 25,000
Liner (501,000 sq ft @ $.687/sq ft)	344,200
Salt (NaCl--24,230 tons @ $20/ton)	484,600
Heat Exchangers	120,000
Piping, Pumps, Misc.	150,000
Fence	30,000
Evaporative Pond Liner (371,000 sq ft @ $.687/sq ft)	254,800
Estimated Labor Cost	230,000
Total	$1,638,600

5. A market survey to investigate the availability of local materials for pond construction and their costs will have to be conducted.
6. The training and education of local engineers will be beneficial for the efficient operation and maintenance of the facility.

Long Term Objective and Future of the Demonstration Pond

Following are some of the gains expected from the demonstration pond:

1. Experience from the first (to our knowledge) of unlined solar pond constructed by dikes on a lake shore. From the viewpoint of the development of solar pond technology, the results would be of global interest.
2. A first hand experience of general construction operation and maintenance of solar ponds in Egypt. Future designs of solar ponds would be based on lessons learned from this facility.
3. Development of the technical skills of native engineers in this, rapidly emerging, field of new energy.
4. Development of new sources of energy and its incorporation in the Egyptian economic and industrial framework.
5. Possible expansion of the demonstration pond into a large solar pond of about 100 km^2 in area at Lake Qarun for power generation.

REFERENCES

1. Tabor, H. (1981) "Review Article Solar Ponds" Solar Energy, Vol. 27, No. 3 pp 181-194

2. Hull, J. R. et al, 1982, "Construction and First Year's Operational Results of the ANL Research Salt Gradient Solar Pond" Proc. AS/ISES Houston, June 1-5, 1982.

3. Wittenberg, L. J. and Etter, D. E. 1982 "Heat Extraction from a large Solar Pond" 1982 Annual Winter Meeting, ASME, Phoenix, Arizona Nov. 15-19. 1982.

4. Tabor, H. (1980) "Non-Connecting Solar Ponds" Phil. Trans. R. Soc. London, A 295 pp 423-433.

5. Tulsa Dist. U. S. Army Corps of Engineers "The Technical and Economic Feasibility of Salt Gradient Solar Ponds at the Truscott Brine Lake, Red River, Chloride Control Project", Sept. 1982.

6. Dake, J. M. K. and Harleman, D. R. F (1969) "Thermal Stratification in Lakes: Analytic and Laboratory Studies," Water Resourc. Res. 5 pp 480-495.

7. Nielson, Carl E. 1981 "Salt Gradient Solar Pond Development", The Ohio State University Research Foundation". Annual DOE Active Solar Heating and Cooling Contractors Review Meeting, March 1980.

8. Rabl A. and C. E. Nielson (1975) "Solar Ponds for Space Heating", Solar Energy 17, pp 1-12.

9. Hull, J. R. (1978), "The effects of Radiation Absorption on Convective Instability in Salt Gradient Solar Ponds", "Proc. Am. Soc. of ISEC Meeting. pp 37-40, Denver, Colorado.

10. Zangrando, F., Bryant, M. C. (1977) "Heat Extraction from a Salt-Gradient Solar Pond", Proceeding Internaitonal Conference on Alternative Energy Sources; Miami Beach, FL Dec. 5-7 1977 Washington D.C. Vol. 6, 2935-2967.

11. Zangrando, F. and H. C. Bryant, (1978) "A Salt Gradient Solar Pond", Solar Age, April 1978, pp 21, 32-36.

12. California Energy Commission, May 1981 "A Study of the feasibility of a Solar Salt Pond Generating facility in the State of California, USA" Final Report Vol. I and II.

13. Hull, J. R. et al (1981) "Dependence of Ground Heat Loss upon Solar Pond Size and Perimeter Insulation - Calculated and Experimental Results." Proc. IBES Cong. Brighton England Aug. 23-28, 1981.

cont--

14. Nielson, C. E. (1976) "Experience with a Prototype Solar Pond for Space Heating", Sharing the Sun, Vol 5 Proc. Joint Conf. Am. and Canadian Solar Energy Soc. Winnipeg, Canada, 1976.

15. Lin et al,(1982) "Regional Applicability and Potential of Salt Gradient Solar Ponds in the United States, Vol II. detailed Report" JPL Publication, 82-10 Vol. II.

16. Bryant, H. C.(1980) "Solar Pond Studies - Phase III" University of New Mexico, EG-77-S-04-3977.

17. Tabor H. and Weinberger, Z. (1980) "Non-Convecting Solar Ponds" Solar Energy Handbook, Kreider McGraw Hill, New York.

18. Zangrando, F. (1980) "A Simple Method to Establish Salt Gradient Solar Ponds", Solar Energy, Vol. 25 No. 5 pp 467-470.

19. Atkinson, J. F. and D. R. F. Harleman,(1982) "A Wind Mixed Model for Solar Ponds" submitted for publication in Solar Energy, Feb. 1982.

20. Edesses Michael (1982) "On Solar Ponds: Salty Fare for the World's Appetite", Technology Review, Vol. 85 No. 8, MIT, Cambridge, USA, pp 58-68.

21. Bloss, S. and Harlemen, D. R. F. (1979) "Effect of Wind Mixing on the Thermocline Formation in Lakes and Reservoirs", Technical Report No. 249. Ralph M. Parsons Laboratory, MIT.

22. Technology Adaptation Program, MIT (1981) "Evaporation And Salinity Studies for the Qattara Depression Project", Progress Report, Sept. 1, 1981 through Nov. 30, 1981.

23. Joint Venture Qattara-Lahmeter International GMBH Salzgetter Consult GMBH, Deutsche Project Union GMBH, 1979 "Study Qattara-Depression" Draft Feasibility Report, Vol. 1, 2 and 3, October 1979.

24. Kuberg Dieter W. "A Review of TVA's Non-convecting Solar Pond Activities" Division of Energy Demonstration and Technology, Tennessee Valley Authority, Chattanooga Tennessee 37401, USA.

25. Solar Energy Research Institute, Solar Ponds - A Selected Bibliography, Report No. SERI/TR-752-711, SEIDB Information Module 8211, Golden, Colo., Nov. 1981.